12 Discrete Hilbert Transforms

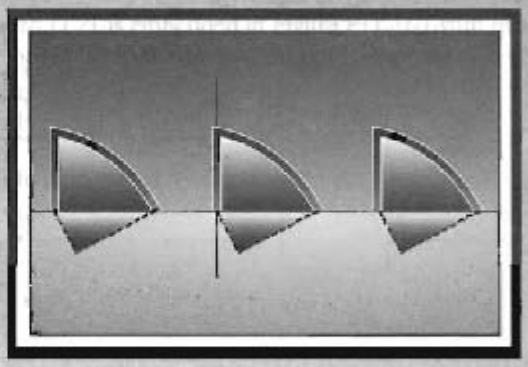

12.0 INTRODUCTION

In general, the specification of the Fourier transform of a sequence requires complete knowledge of both the real and imaginary parts or of the magnitude and phase at all frequencies in the range $-\pi < \omega \leq \pi$. However, we have seen that under certain conditions, there are constraints on the Fourier transform. For example, in Section 2.8, we saw that if $x[n]$ is real, then its Fourier transform is conjugate symmetric, i.e., $X(e^{j\omega}) = X^*(e^{-j\omega})$. From this, it follows that for real sequences, specification of $X(e^{j\omega})$ for $0 \leq \omega \leq \pi$ also specifies it for $-\pi \leq \omega \leq 0$. Similarly, we saw in Section 5.4 that under the constraint of minimum phase, the Fourier transform magnitude and phase are not independent; i.e., specification of magnitude determines the phase and specification of phase determines the magnitude to within a scale factor. In Section 8.5, we saw that for sequences of finite length N, specification of $X(e^{j\omega})$ at N equally spaced frequencies determines $X(e^{j\omega})$ at all frequencies.

In this chapter, we will see that the constraint of causality of a sequence implies unique relationships between the real and imaginary parts of the Fourier transform. Relationships of this type between the real and imaginary parts of complex functions arise in many fields besides signal processing, and they are commonly known as *Hilbert transform relationships*. In addition to developing these relationships for the Fourier transform of causal sequences, we will develop related results for the DFT and for sequences with one-sided Fourier transforms. Also, in Section 12.3 we will indicate how the relationship between magnitude and phase for minimum-phase sequences can be interpreted in terms of the Hilbert transform.

Although we will take an intuitive approach in this chapter (see Gold, Oppenheim and Rader, 1970) it is important to be aware that the Hilbert transform relationships follow formally from the properties of analytic functions. (See Problem 12.21.) Specifically, the complex functions that arise in the mathematical representation of discrete-time signals and systems are generally very well-behaved functions. With few exceptions, the z-transforms that have concerned us have had well-defined regions in which the power series is absolutely convergent. Since a power series represents an analytic function within its ROC, it follows that z-transforms are analytic functions inside their ROCs. By the definition of an analytic function, this means that the z-transform has a well-defined derivative at every point inside the ROC. Furthermore, for analytic functions the z-transform and all its derivatives are continuous functions within the ROC.

The properties of analytic functions imply some rather powerful constraints on the behavior of the z-transform within its ROC. Since the Fourier transform is the z-transform evaluated on the unit circle, these constraints also restrict the behavior of the Fourier transform. One such constraint is that the real and imaginary parts satisfy the Cauchy–Riemann conditions, which relate the partial derivatives of the real and imaginary parts of an analytic function. (See, for example, Churchill and Brown, 1990.) Another constraint is the Cauchy integral theorem, through which the value of a complex function is specified everywhere inside a region of analyticity in terms of the values of the function on the boundary of the region. On the basis of these relations for analytic functions, it is possible, under certain conditions, to derive explicit integral relationships between the real and imaginary parts of a z-transform on a closed contour within the ROC. In the mathematics literature, these relations are often referred to as *Poisson's formulas*. In the context of system theory, they are known as the *Hilbert transform relations*.

Rather than following the mathematical approach just discussed, we will develop the Hilbert transform relations by exploiting the fact that the real and imaginary parts of the Fourier transform of a causal sequence are the transforms of the even and odd components, respectively, of the sequence (properties 5 and 6, Table 2.1). As we will show, a causal sequence is completely specified by its even part, implying that the Fourier transform of the original sequence is completely specified by its real part. In addition to applying this argument to specifying the Fourier transform of a particular causal sequence in terms of its real part, we can also apply it, under certain conditions, to specify the Fourier transform of a sequence in terms of its magnitude.

The notion of an analytic signal is an important concept in continuous-time signal processing. An analytic signal is a complex time function (which is analytic) having a Fourier transform that vanishes for negative frequencies. A complex sequence cannot be considered in any formal sense to be analytic, since it is a function of an integer variable. However, in a style similar to that described in the previous paragraph, it is possible to relate the real and imaginary parts of a complex sequence whose spectrum is zero on the unit circle for $-\pi < \omega < 0$. A similar approach can also be taken in relating the real and imaginary parts of the DFT for a periodic or, equivalently, a finite-length sequence. In this case, the "causality" condition is that the periodic sequence be zero in the second half of each period.

Thus, in this chapter, a notion of causality will be applied to relate the even and odd components of a function or, equivalently, the real and imaginary parts of its transform. We will apply this approach in four situations. First, we relate the real and imaginary parts of the Fourier transform $X(e^{j\omega})$ of a sequence $x[n]$ that is zero for $n < 0$. In the second situation, we obtain a relationship between the real and imaginary parts of the DFT for periodic sequences or, equivalently, for a finite-length sequence considered to be of length N, but with the last $(N/2) - 1$ points restricted to zero. In the third case, we relate the real and imaginary parts of the *logarithm* of the Fourier transform under the condition that the inverse transform of the logarithm of the transform is zero for $n < 0$. Relating the real and imaginary parts of the logarithm of the Fourier transform corresponds to relating the log magnitude and phase of $X(e^{j\omega})$. Finally, we relate the real and imaginary parts of a complex sequence whose Fourier transform, considered as a periodic function of ω, is zero in the second half of each period.

12.1 REAL- AND IMAGINARY-PART SUFFICIENCY OF THE FOURIER TRANSFORM FOR CAUSAL SEQUENCES

Any sequence can be expressed as the sum of an even sequence and an odd sequence. Specifically, with $x_e[n]$ and $x_o[n]$ denoting the even and odd parts, respectively, of $x[n]$,[1] we have

$$x[n] = x_e[n] + x_o[n], \tag{12.1}$$

where

$$x_e[n] = \frac{x[n] + x[-n]}{2} \tag{12.2}$$

and

$$x_o[n] = \frac{x[n] - x[-n]}{2}. \tag{12.3}$$

Equations (12.1) to (12.3) apply to an arbitrary sequence, whether or not it is causal and whether or not it is real. However, if $x[n]$ is causal, i.e., if $x[n] = 0, n < 0$, then it is possible to recover $x[n]$ from $x_e[n]$ or to recover $x[n]$ for $n \neq 0$ from $x_o[n]$. Consider, for example, the causal sequence $x[n]$ and its even and odd components, as shown in Figure 12.1. Because $x[n]$ is causal, $x[n] = 0$ for $n < 0$ and $x[-n] = 0$ for $n > 0$. Therefore, the nonzero portions of $x[n]$ and $x[-n]$ do not overlap except at $n = 0$. For this reason, it follows from Eqs. (12.2) and (12.3) that

$$x[n] = 2x_e[n]u[n] - x_e[0]\delta[n] \tag{12.4}$$

and

$$x[n] = 2x_o[n]u[n] + x[0]\delta[n]. \tag{12.5}$$

The validity of these relationships is easily seen in Figure 12.1. Note that $x[n]$ is completely determined by $x_e[n]$. On the other hand, $x_o[0] = 0$, so we can recover $x[n]$ from $x_o[n]$ only for $n \neq 0$.

[1] If $x[n]$ is real, then $x_e[n]$ and $x_o[n]$ in Eqs. (12.2) and (12.3) are the even and odd parts, respectively, of $x[n]$ as considered in Chapter 2. If $x[n]$ is complex, for the purposes of this discussion we still define $x_e[n]$ and $x_o[n]$ as in Eqs. (12.2) and (12.3), which do not correspond to the conjugate-symmetric and conjugate-antisymmetric parts of a complex sequence as considered in Chapter 2.

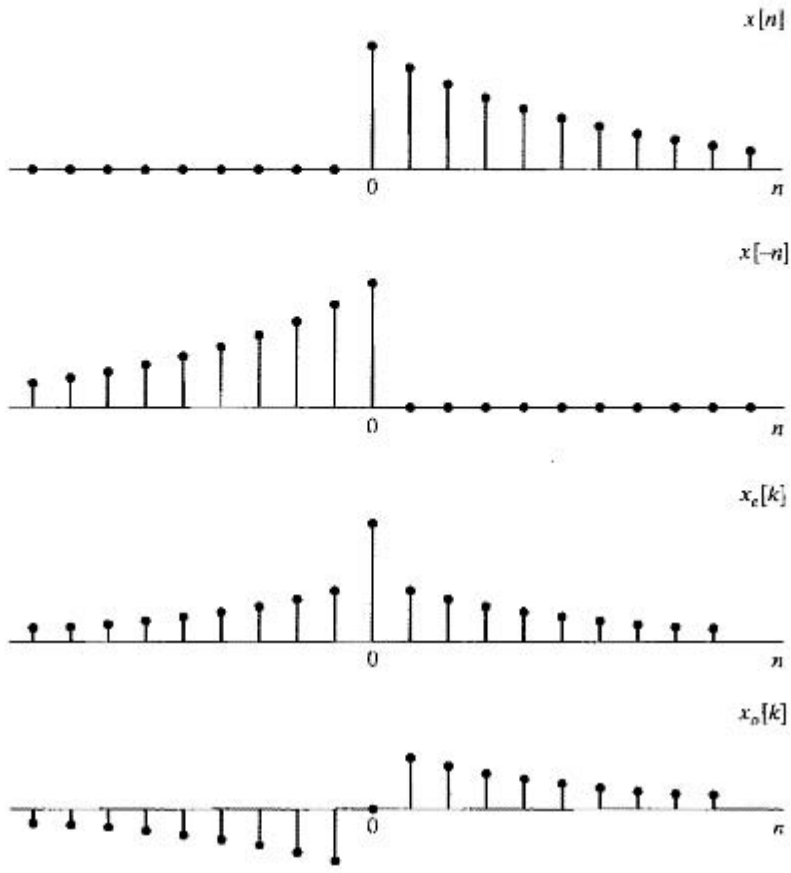

Figure 12.1 Even and odd parts of a real causal sequence.

Now, if $x[n]$ is also stable, i.e., absolutely summable, then its Fourier transform exists. We denote the Fourier transform of $x[n]$ as

$$X(e^{j\omega}) = X_R(e^{j\omega}) + jX_I(e^{j\omega}), \tag{12.6}$$

where $X_R(e^{j\omega})$ is the real part and $X_I(e^{j\omega})$ is the imaginary part of $X(e^{j\omega})$. Recall that if $x[n]$ is a *real* sequence, then $X_R(e^{j\omega})$ is the Fourier transform of $x_e[n]$ and $jX_I(e^{j\omega})$ is the Fourier transform of $x_o[n]$. Therefore, for a *causal, stable, real* sequence, $X_R(e^{j\omega})$ completely determines $X(e^{j\omega})$, since, if we are given $X_R(e^{j\omega})$, we can find $X(e^{j\omega})$ by the following process:

1. Find $x_e[n]$ as the inverse Fourier transform of $X_R(e^{j\omega})$.
2. Find $x[n]$ using Eq. (12.4).
3. Find $X(e^{j\omega})$ as the Fourier transform of $x[n]$.

This also implies, of course, that $X_I(e^{j\omega})$ can be determined from $X_R(e^{j\omega})$. In Example 12.1, we illustrate how this procedure can be applied to obtain $X(e^{j\omega})$ and $X_I(e^{j\omega})$ from $X_R(e^{j\omega})$.

Example 12.1 Finite-Length Sequence

Consider a real, causal sequence $x[n]$ for which $X_R(e^{j\omega})$, the real part of the DTFT, is

$$X_R(e^{j\omega}) = 1 + \cos 2\omega. \tag{12.7}$$

We would like to determine the original sequence $x[n]$, its Fourier transform $X(e^{j\omega})$, and the imaginary part of the Fourier transform, $X_I(e^{j\omega})$. As a first step, we rewrite Eq. (12.7) expressing the cosine as a sum of complex exponentials:

$$X_R(e^{j\omega}) = 1 + \frac{1}{2}e^{-j2\omega} + \frac{1}{2}e^{j2\omega}. \tag{12.8}$$

We know that $X_R(e^{j\omega})$ is the Fourier transform of $x_e[n]$, the even part of $x[n]$ as defined in Eq. (12.2). Comparing Eq. (12.8) with the definition of the Fourier transform, Eq. (2.131), we can match terms to obtain

$$x_e[n] = \delta[n] + \frac{1}{2}\delta[n-2] + \frac{1}{2}\delta[n+2].$$

Now that we have obtained the even part, we can use the relation in Eq. (12.4) to obtain

$$x[n] = \delta[n] + \delta[n-2]. \tag{12.9}$$

From $x[n]$, we get

$$\begin{aligned} X(e^{j\omega}) &= 1 + e^{-j2\omega} \\ &= 1 + \cos 2\omega - j \sin 2\omega. \end{aligned} \tag{12.10}$$

From Eq. (12.10), we can both confirm that $X_R(e^{j\omega})$ is as specified in Eq. (12.7) and also obtain

$$X_I(e^{j\omega}) = -\sin 2\omega. \tag{12.11}$$

As an alternative path to obtaining $X_I(e^{j\omega})$, we can first use Eq. (12.3) to get $x_o[n]$ from $x[n]$. Substituting Eq. (12.9) into Eq. (12.3) then yields

$$x_o[n] = \frac{1}{2}\delta[n-2] - \frac{1}{2}\delta[n+2].$$

The Fourier transform of $x_o[n]$ is $jX_I(e^{j\omega})$, so we find

$$\begin{aligned} jX_I(e^{j\omega}) &= \frac{1}{2}e^{-j2\omega} - \frac{1}{2}e^{j2\omega} \\ &= -j \sin 2\omega, \end{aligned}$$

so that

$$X_I(e^{j\omega}) = -\sin 2\omega,$$

which is consistent with Eq. (12.11).

Example 12.2 Exponential Sequence

Let

$$X_R(e^{j\omega}) = \frac{1 - \alpha\cos\omega}{1 - 2\alpha\cos\omega + \alpha^2}, \qquad |\alpha| < 1, \tag{12.12}$$

or equivalently,

$$X_R(e^{j\omega}) = \frac{1 - (\alpha/2)(e^{j\omega} + e^{-j\omega})}{1 - \alpha(e^{j\omega} + e^{-j\omega}) + \alpha^2}, \qquad |\alpha| < 1, \tag{12.13}$$

with α real. We first determine $x_e[n]$ and then $x[n]$ using Eq. (12.4).

To obtain $x_e[n]$, the inverse Fourier transform of $X_R(e^{j\omega})$, it is convenient to first obtain $X_R(z)$, the z-transform of $x_e[n]$. This follows directly from Eq. (12.13), given that

$$X_R(e^{j\omega}) = X_R(z)\big|_{z=e^{j\omega}}.$$

Consequently, by replacing $e^{j\omega}$ by z in Eq. (12.13), we obtain

$$X_R(z) = \frac{1 - (\alpha/2)(z + z^{-1})}{1 - \alpha(z + z^{-1}) + \alpha^2} \tag{12.14}$$

$$= \frac{1 - \frac{\alpha}{2}(z + z^{-1})}{(1 - \alpha z^{-1})(1 - \alpha z)}. \tag{12.15}$$

Since we began with the Fourier transform $X_R(e^{j\omega})$ and obtained $X_R(z)$ by extending $X_R(e^{j\omega})$ into the z-plane, the ROC of $X_R(z)$ must, of course, include the unit circle and is then bounded on the inside by the pole at $z = \alpha$ and on the outside by the pole at $z = 1/\alpha$.

From Eq. (12.15), we now want to obtain $x_e[n]$, the inverse z-transform of $X_R(z)$. We do this by expanding Eq. (12.15) in partial fractions, yielding

$$X_R(z) = \frac{1}{2}\left[\frac{1}{1 - \alpha z^{-1}} + \frac{1}{1 - \alpha z}\right], \tag{12.16}$$

with the ROC specified to include the unit circle. The inverse z-transform of Eq. (12.16) can then be applied separately to each term to obtain

$$x_e[n] = \frac{1}{2}\alpha^n u[n] + \frac{1}{2}\alpha^{-n}u[-n]. \tag{12.17}$$

Consequently, from Eq. (12.4),

$$\begin{aligned} x[n] &= \alpha^n u[n] + \alpha^{-n}u[-n]u[n] - \delta[n] \\ &= \alpha^n u[n]. \end{aligned}$$

$X(e^{j\omega})$ is then given by

$$X(e^{j\omega}) = \frac{1}{1 - \alpha e^{-j\omega}}, \tag{12.18}$$

and $X(z)$ is given by

$$X(z) = \frac{1}{1 - \alpha z^{-1}} \qquad |z| > |\alpha|. \tag{12.19}$$

The constructive procedure illustrated in Example 12.1 can be interpreted analytically to obtain a general relationship that expresses $X_I(e^{j\omega})$ directly in terms of $X_R(e^{j\omega})$. From Eq. (12.4), the complex convolution theorem, and the fact that $x_e[0] = x[0]$, it follows that

$$X(e^{j\omega}) = \frac{1}{\pi}\int_{-\pi}^{\pi} X_R(e^{j\theta})U(e^{j(\omega-\theta)})d\theta - x[0], \tag{12.20}$$

where $U(e^{j\omega})$ is the Fourier transform of the unit step sequence. As stated in Section 2.7, although the unit step is neither absolutely summable nor square summable, it can be represented by the Fourier transform

$$U(e^{j\omega}) = \sum_{k=-\infty}^{\infty} \pi\delta(\omega - 2\pi k) + \frac{1}{1-e^{-j\omega}}, \tag{12.21}$$

or, since the term $1/(1 - e^{-j\omega})$ can be rewritten as

$$\frac{1}{1-e^{-j\omega}} = \frac{1}{2} - \frac{j}{2}\cot\left(\frac{\omega}{2}\right), \tag{12.22}$$

Eq. (12.21) becomes

$$U(e^{j\omega}) = \sum_{k=-\infty}^{\infty} \pi\delta(\omega - 2\pi k) + \frac{1}{2} - \frac{j}{2}\cot\left(\frac{\omega}{2}\right). \tag{12.23}$$

Using Eq. (12.23), we can express Eq. (12.20) as

$$\begin{aligned} X(e^{j\omega}) &= X_R(e^{j\omega}) + jX_I(e^{j\omega}) \\ &= X_R(e^{j\omega}) + \frac{1}{2\pi}\int_{-\pi}^{\pi} X_R(e^{j\theta})d\theta \\ &\quad - \frac{j}{2\pi}\int_{-\pi}^{\pi} X_R(e^{j\theta})\cot\left(\frac{\omega-\theta}{2}\right)d\theta - x[0]. \end{aligned} \tag{12.24}$$

Equating real and imaginary parts in Eq. (12.24) and noting that

$$x[0] = \frac{1}{2\pi}\int_{-\pi}^{\pi} X_R(e^{j\theta})d\theta, \tag{12.25}$$

we obtain the relationship

$$X_I(e^{j\omega}) = -\frac{1}{2\pi}\int_{-\pi}^{\pi} X_R(e^{j\theta})\cot\left(\frac{\omega-\theta}{2}\right)d\theta. \tag{12.26}$$

A similar procedure can be followed to obtain $x[n]$ and $X(e^{j\omega})$ from $X_I(e^{j\omega})$ and $x[0]$ using Eq. (12.5). This process results in the following equation for $X_R(e^{j\omega})$ in terms of $X_I(e^{j\omega})$:

$$X_R(e^{j\omega}) = x[0] + \frac{1}{2\pi}\int_{-\pi}^{\pi} X_I(e^{j\theta})\cot\left(\frac{\omega-\theta}{2}\right)d\theta. \tag{12.27}$$

Equations (12.26) and (12.27), which are called *discrete Hilbert transform relationships*, hold for the real and imaginary parts of the Fourier transform of a causal, stable, real sequence. They are improper integrals, since the integrand is singular at

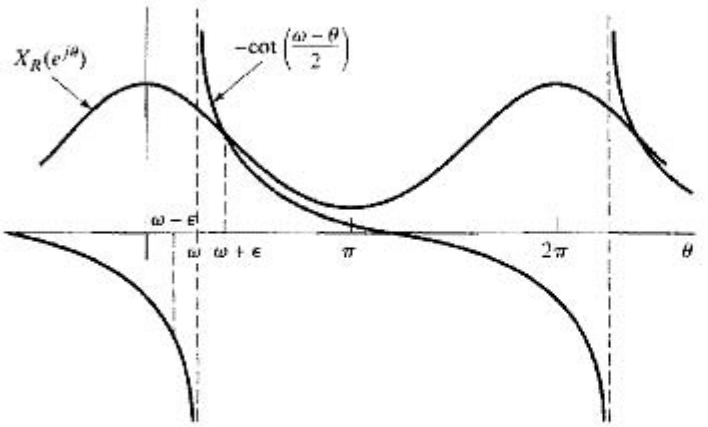

Figure 12.2 Interpretation of the Hilbert transform as a periodic convolution.

$\omega - \theta = 0$. Such integrals must be evaluated carefully to obtain a consistent finite result. This can be done formally by interpreting the integrals as *Cauchy principal values*. That is, Eq. (12.26) becomes

$$X_I(e^{j\omega}) = -\frac{1}{2\pi}\mathcal{P}\int_{-\pi}^{\pi} X_R(e^{j\theta})\cot\left(\frac{\omega-\theta}{2}\right)d\theta. \tag{12.28a}$$

and Eq. (12.27) becomes

$$X_R(e^{j\omega}) = x[0] + \frac{1}{2\pi}\mathcal{P}\int_{-\pi}^{\pi} X_I(e^{j\theta})\cot\left(\frac{\omega-\theta}{2}\right)d\theta, \tag{12.28b}$$

where $\mathcal{P}$ denotes the Cauchy principal value of the integral that follows. The meaning of the Cauchy principal value in Eq. (12.28a), for example, is

$$X_I(e^{j\omega}) = -\frac{1}{2\pi}\lim_{\varepsilon\to 0}\left[\int_{\omega+\varepsilon}^{\pi} X_R(e^{j\theta})\cot\left(\frac{\omega-\theta}{2}\right)d\theta + \int_{-\pi}^{\omega-\varepsilon} X_R(e^{j\theta})\cot\left(\frac{\omega-\theta}{2}\right)d\theta\right]. \tag{12.29}$$

Equation (12.29) shows that $X_I(e^{j\omega})$ is obtained by the periodic convolution of $-\cot(\omega/2)$ with $X_R(e^{j\omega})$, with special care being taken in the vicinity of the singularity at $\theta = \omega$. In a similar manner, Eq. (12.28b) involves the periodic convolution of $\cot(\omega/2)$ with $X_I(e^{j\omega})$.

The two functions involved in the convolution integral of Eq. (12.28a) or, equivalently, Eq. (12.29) are illustrated in Figure 12.2. The limit in Eq. (12.29) exists because the function $\cot[(\omega-\theta)/2]$ is antisymmetric at the singular point $\theta = \omega$ and the limit is taken symmetrically about the singularity.

12.2 SUFFICIENCY THEOREMS FOR FINITE-LENGTH SEQUENCES

In Section 12.1, we showed that causality or one-sidedness of a real sequence implies some strong constraints on the Fourier transform of the sequence. The results of the

previous section apply, of course, to finite-length causal sequences, but since the finite-length property is more restrictive, it is perhaps reasonable to expect the Fourier transform of a finite-length sequence to be more constrained. We will see that this is indeed the case.

One way to take advantage of the finite-length property is to recall that finite-length sequences can be represented by the DFT. Since the DFT involves sums rather than integrals, the problems associated with improper integrals disappear.

Since the DFT is, in reality, a representation of a periodic sequence, any results we obtain must be based on corresponding results for periodic sequences. Indeed, it is important to keep the inherent periodicity of the DFT firmly in mind in deriving the desired Hilbert transform relation for finite-length sequences. Therefore, we will consider the periodic case first and then discuss the application to the finite-length case.

Consider a periodic sequence $\tilde{x}[n]$ with period N that is related to a finite-length sequence $x[n]$ of length N by

$$\tilde{x}[n] = x[((n))_N]. \tag{12.30}$$

As in Section 12.1, $\tilde{x}[n]$ can be represented as the sum of an even and odd periodic sequence,

$$\tilde{x}[n] = \tilde{x}_e[n] + \tilde{x}_o[n], \qquad n = 0, 1, \ldots, (N-1), \tag{12.31}$$

where

$$\tilde{x}_e[n] = \frac{\tilde{x}[n] + \tilde{x}[-n]}{2}, \qquad n = 0, 1, \ldots, (N-1), \tag{12.32a}$$

and

$$\tilde{x}_o[n] = \frac{\tilde{x}[n] - \tilde{x}[-n]}{2}, \qquad n = 0, 1, \ldots, (N-1). \tag{12.32b}$$

A periodic sequence cannot, of course, be causal in the sense used in Section 12.1. We can, however, define a "periodically causal" sequence to be a periodic sequence for which $\tilde{x}[n] = 0$ for $N/2 < n < N$. That is, $\tilde{x}[n]$ is identically zero over the last half of the period. We assume henceforth that N is even; the case of N odd is considered in Problem 12.25. Note that because of the periodicity of $\tilde{x}[n]$, it is also true that $\tilde{x}[n] = 0$ for $-N/2 < n < 0$. For finite-length sequences, this restriction means that although the sequence is considered to be of length N, the last $(N/2) - 1$ points are in fact zero. In Figure 12.3, we show an example of a periodically causal sequence and its even and odd parts with $N = 8$. Because $\tilde{x}[n]$ is zero in the second half of each period, $\tilde{x}[-n]$ is zero in the first half of each period, and, consequently, except for $n = 0$ and $n = N/2$, there is no overlap between the nonzero portions of $\tilde{x}[n]$ and $\tilde{x}[-n]$. Therefore, for periodically causal periodic sequences,

$$\tilde{x}[n] = \begin{cases} 2\tilde{x}_e[n], & n = 1, 2, \ldots, (N/2) - 1, \\ \tilde{x}_e[n], & n = 0, N/2, \\ 0, & n = (N/2) + 1, \ldots, N - 1, \end{cases} \tag{12.33}$$

and

$$\tilde{x}[n] = \begin{cases} 2\tilde{x}_o[n], & n = 1, 2, \ldots, (N/2) - 1, \\ 0, & n = (N/2) + 1, \ldots, N - 1, \end{cases} \tag{12.34}$$

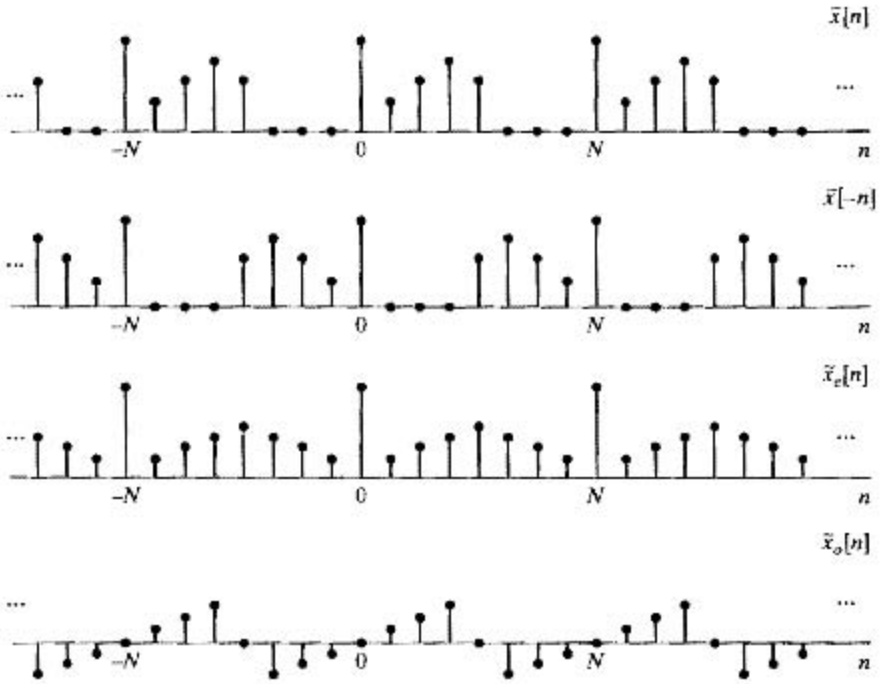

Figure 12.3 Even and odd parts of a periodically causal, real, periodic sequence of period $N = 8$.

where $\tilde{x}[n]$ cannot be recovered from $\tilde{x}_o[n]$ because $\tilde{x}_o[0] = \tilde{x}_o[N/2] = 0$. If we define the periodic sequence

$$\tilde{u}_N[n] = \begin{cases} 1, & n = 0, N/2, \\ 2, & n = 1, 2, \ldots, (N/2) - 1, \\ 0, & n = (N/2) + 1, \ldots, N - 1, \end{cases} \tag{12.35}$$

then it follows that, for N even, we can express $\tilde{x}[n]$ as

$$\tilde{x}[n] = \tilde{x}_e[n]\tilde{u}_N[n] \tag{12.36}$$

and

$$\tilde{x}[n] = \tilde{x}_o[n]\tilde{u}_N[n] + \tilde{x}[0]\tilde{\delta}[n] + \tilde{x}[N/2]\tilde{\delta}[n - (N/2)], \tag{12.37}$$

where $\tilde{\delta}[n]$ is a periodic unit-impulse sequence with period N. Thus, the sequence $\tilde{x}[n]$ can be completely recovered from $\tilde{x}_e[n]$. On the other hand, $\tilde{x}_o[n]$ will always be zero at $n = 0$ and $n = N/2$, and consequently, $\tilde{x}[n]$ can be recovered from $\tilde{x}_o[n]$ only for $n \neq 0$ and $n \neq N/2$.

If $\tilde{x}[n]$ is a real periodic sequence of period N with DFS $\tilde{X}[k]$, then $\tilde{X}_R[k]$, the real part of $\tilde{X}[k]$, is the DFS of $\tilde{x}_e[n]$ and $j\tilde{X}_I[k]$ is the DFS of $\tilde{x}_o[n]$. Hence, Eqs. (12.36) and (12.37) imply that, for a periodic sequence of period N, which is periodically causal in the sense defined earlier, $\tilde{X}[k]$ can be recovered from its real part or (almost) from its imaginary part. Equivalently, $\tilde{X}_I[k]$ can be obtained from $\tilde{X}_R[k]$, and $\tilde{X}_R[k]$ can (almost) be obtained from $\tilde{X}_I[k]$.

Specifically, suppose that we are given $\tilde{X}_R[k]$. Then, we can obtain $\tilde{X}[k]$ and $\tilde{X}_I[k]$ by the following procedure:

1. Compute $\tilde{x}_e[n]$ using the DFS synthesis equation

$$\tilde{x}_e[n] = \frac{1}{N}\sum_{k=0}^{N-1} \tilde{X}_R[k]e^{j(2\pi/N)kn}. \tag{12.38}$$

2. Compute $\tilde{x}[n]$ using Eq. (12.36).
3. Compute $\tilde{X}[k]$ using the DFS analysis equation

$$\tilde{X}[k] = \sum_{n=0}^{N-1} \tilde{x}[n]e^{-j(2\pi/N)kn} = \tilde{X}_R[k] + j\tilde{X}_I[k]. \tag{12.39}$$

In contrast to the general causal case discussed in Section 12.1, the procedure just outlined can be implemented on a computer, since Eqs. (12.38) and (12.39) can be evaluated accurately and efficiently using an FFT algorithm.

To obtain an explicit relation between $\tilde{X}_R[k]$, and $\tilde{X}_I[k]$, we can carry out the procedure analytically. From Eq. (12.36) and Eq. (8.34), it follows that

$$\begin{aligned}\tilde{X}[k] &= \tilde{X}_R[k] + j\tilde{X}_I[k] \\ &= \frac{1}{N}\sum_{m=0}^{N-1} \tilde{X}_R[m]\tilde{U}_N[k-m];\end{aligned} \tag{12.40}$$

i.e., $\tilde{X}[k]$ is the periodic convolution of $\tilde{X}_R[k]$, the DFS of $\tilde{x}_e[n]$, with $\tilde{U}_N[k]$ the DFS of $\tilde{u}_N[n]$. The DFS of $\tilde{u}_N[n]$ can be shown to be (see Problem 12.24)

$$\tilde{U}_N[k] = \begin{cases} N, & k = 0, \\ -j2\cot(\pi k/N), & k \text{ odd}, \\ 0, & k \text{ even}. \end{cases} \tag{12.41}$$

If we define

$$\tilde{V}_N[k] = \begin{cases} -j2\cot(\pi k/N), & k \text{ odd}, \\ 0, & k \text{ even}, \end{cases} \tag{12.42}$$

then Eq. (12.40) can be expressed as

$$\tilde{X}[k] = \tilde{X}_R[k] + \frac{1}{N}\sum_{m=0}^{N-1} \tilde{X}_R[m]\tilde{V}_N[k-m]. \tag{12.43}$$

Therefore,

$$j\tilde{X}_I[k] = \frac{1}{N}\sum_{m=0}^{N-1} \tilde{X}_R[m]\tilde{V}_N[k-m], \tag{12.44}$$

which is the desired relation between the real and imaginary parts of the DFS of a periodically causal, real, and periodic sequence. Similarly, beginning with Eq. (12.37) we can show that

$$\tilde{X}_R[k] = \frac{1}{N}\sum_{m=0}^{N-1} j\tilde{X}_I[m]\tilde{V}_N[k-m] + \tilde{x}[0] + (-1)^k\tilde{x}[N/2]. \tag{12.45}$$

Equations (12.44) and (12.45) relate the real and imaginary parts of the DFS representation of the periodic sequence $\tilde{x}[n]$. If $\tilde{x}[n]$ is thought of as the periodic repetition of a finite-length sequence $x[n]$ as in Eq. (12.30), then

$$x[n] = \begin{cases} \tilde{x}[n], & 0 \le n \le N-1, \\ 0, & \text{otherwise.} \end{cases} \tag{12.46}$$

If $x[n]$ has the "periodic causality" property with respect to a period N (i.e., $x[n] = 0$ for $n < 0$ and for $n > N/2$), then all of the preceding discussion applies to the DFT of $x[n]$. In other words, we can remove the tildes from Eqs. (12.44) and (12.45), thereby obtaining the DFT relations

$$jX_I[k] = \begin{cases} \dfrac{1}{N}\displaystyle\sum_{m=0}^{N-1} X_R[m]V_N[k-m], & 0 \le k \le N-1, \\ 0, & \text{otherwise,} \end{cases} \tag{12.47}$$

and

$$X_R[k] = \begin{cases} \dfrac{1}{N}\displaystyle\sum_{m=0}^{N-1} jX_I[m]V_N[k-m] + x[0] + (-1)^k x[N/2], & 0 \le k \le N-1, \\ 0, & \text{otherwise.} \end{cases} \tag{12.48}$$

Note that the sequence $V_N[k-m]$ given by Eq. (12.42) is periodic with period N, so we do not need to worry about computing $((k-m))_N$ in Eqs. (12.47) and (12.48), which are the desired relations between the real and imaginary parts of the N-point DFT of a real sequence whose actual length is less than or equal to $(N/2)+1$ (for N even). These equations are circular convolutions, and, for example, Eq. (12.47) can be evaluated efficiently by the following procedure:

1. Compute the inverse DFT of $X_R[k]$ to obtain the sequence

$$x_{ep}[n] = \frac{x[n] + x[((-n))_N]}{2}, \qquad 0 \le n \le N-1. \tag{12.49}$$

2. Compute the periodic odd part of $x[n]$ by

$$x_{op}[n] = \begin{cases} x_{ep}[n], & 0 < n < N/2, \\ -x_{ep}[n], & N/2 < n \le N-1, \\ 0, & \text{otherwise.} \end{cases} \tag{12.50}$$

3. Compute the DFT of $x_{op}[n]$ to obtain $jX_I[k]$.

Note that if, instead of computing the odd part of $x[n]$ in step 2, we compute

$$x[n] = \begin{cases} x_{ep}[0], & n = 0, \\ 2x_{ep}[n], & 0 < n < N/2, \\ x_{ep}[N/2], & n = N/2, \\ 0, & \text{otherwise,} \end{cases} \tag{12.51}$$

then the DFT of the resulting sequence would be $X[k]$, the complete DFT of $x[n]$.

Example 12.3 Periodic Sequence

Consider a sequence that is periodically causal with period $N = 4$ and that has

$$X_R[k] = \begin{cases} 2, & k = 0, \\ 3, & k = 1, \\ 4, & k = 2, \\ 3, & k = 3. \end{cases}$$

We can find the imaginary part of the DFT in one of two ways. The first way is to use Eq. (12.47). For $N = 4$,

$$V_4[k] = \begin{cases} 2j, & k = -1 + 4m, \\ -2j, & k = 1 + 4m, \\ 0, & \text{otherwise}, \end{cases}$$

where m is an integer. Implementing the convolution in Eq. (12.47) yields

$$jX_I[k] = \frac{1}{4}\sum_{m=0}^{3} X_R[m]V_4[k-m], \qquad 0 \le k \le 3$$

$$= \begin{cases} j, & k = 1, \\ -j, & k = 3, \\ 0, & \text{otherwise}. \end{cases}$$

Alternatively, we can follow the three-step procedure that includes Eqs. (12.49) and (12.50). Computing the inverse DFT $X_R[k]$ yields

$$x_e[n] = \frac{1}{4}\sum_{k=0}^{3} X_R[k]W_4^{-kn} = \frac{1}{4}[2 + 3(j)^n + 4(-1)^n + 3(-j)^n]$$

$$= \begin{cases} 3, & n = 0, \\ -\frac{1}{2}, & n = 1, 3, \\ 0, & n = 2. \end{cases}$$

Note that although this sequence is not itself even symmetric, a periodic replication of $x_e[n]$ is even symmetric. Thus, the DFT $X_R[k]$ of $x_e[n]$ is purely real. Equation (12.50) allows us to find the periodically odd part $x_{\text{op}}[n]$; specifically,

$$x_{\text{op}}[n] = \begin{cases} -\frac{1}{2}, & n = 1, \\ \frac{1}{2}, & n = 3, \\ 0, & \text{otherwise}. \end{cases}$$

Finally, we obtain $jX_I[k]$ from the DFT of $x_{\text{op}}[n]$:

$$jX_I[k] = \sum_{n=0}^{3} x_{\text{op}}[n]W_4^{nk} = -\frac{1}{2}W_4^k + \frac{1}{2}W_4^{3k}$$

$$= \begin{cases} j, & k = 1, \\ -j, & k = 3, \\ 0, & \text{otherwise}, \end{cases}$$

which is, of course, the same as was obtained from Eq. (12.47).

12.3 RELATIONSHIPS BETWEEN MAGNITUDE AND PHASE

So far, we have focused on the relationships between the real and imaginary parts of the Fourier transform of a sequence. Often, we are interested in relationships between the magnitude and phase of the Fourier transform. In this section, we consider the conditions under which these functions might be uniquely related. Although it might appear on the surface that a relationship between real and imaginary parts implies a relationship between magnitude and phase, that is not the case. This is clearly demonstrated by Example 5.9 in Section 5.4. The two system functions $H_1(z)$ and $H_2(z)$ in that example were assumed to correspond to causal, stable systems. Therefore, the real and imaginary parts of $H_1(e^{j\omega})$ are related through the Hilbert transform relations of Eqs. (12.28a) and (12.28b), as are the real and imaginary parts of $H_2(e^{j\omega})$. However, $\angle H_1(e^{j\omega})$ could not be obtained from $|H_1(e^{j\omega})|$, since $H_1(e^{j\omega})$ and $H_2(e^{j\omega})$ have the same magnitude but a different phase.

The Hilbert transform relationship between the real and imaginary parts of the Fourier transform of a sequence $x[n]$ was based on the causality of $x[n]$. We can obtain a Hilbert transform relationship between magnitude and phase by imposing causality on a sequence $\hat{x}[n]$ derived from $x[n]$ for which the Fourier transform $\hat{X}(e^{j\omega})$ is the logarithm of the Fourier transform of $x[n]$. Specifically, we define $\hat{x}[n]$ so that

$$x[n] \xleftrightarrow{\mathcal{F}} X(e^{j\omega}) = |X(e^{j\omega})|e^{j\arg[X(e^{j\omega})]}, \tag{12.52a}$$

$$\hat{x}[n] \xleftrightarrow{\mathcal{F}} \hat{X}(e^{j\omega}), \tag{12.52b}$$

where

$$\hat{X}(e^{j\omega}) = \log[X(e^{j\omega})] = \log|X(e^{j\omega})| + j\arg[X(e^{j\omega})] \tag{12.53}$$

and, as defined in Section 5.1, $\arg[X(e^{j\omega})]$ denotes the continuous phase of $X(e^{j\omega})$. The sequence $\hat{x}[n]$ is commonly referred to as the *complex cepstrum* of $x[n]$, the properties and applications of which are discussed in detail in Chapter 13.[2]

If we now require that $\hat{x}[n]$ be causal, then the real and imaginary parts of $\hat{X}(e^{j\omega})$, corresponding to $\log|X(e^{j\omega})|$ and $\arg[X(e^{j\omega})]$, respectively, will be related through Eqs. (12.28a) and (12.28b); i.e.,

$$\arg[X(e^{j\omega})] = -\frac{1}{2\pi}\mathcal{P}\int_{-\pi}^{\pi}\log|X(e^{j\theta})|\cot\left(\frac{\omega-\theta}{2}\right)d\theta \tag{12.54}$$

and

$$\log|X(e^{j\omega})| = \hat{x}[0] + \frac{1}{2\pi}\mathcal{P}\int_{-\pi}^{\pi}\arg[X(e^{j\theta})]\cot\left(\frac{\omega-\theta}{2}\right)d\theta, \tag{12.55a}$$

where, in Eq. (12.55a), $\hat{x}[0]$ is

$$\hat{x}[0] = \frac{1}{2\pi}\int_{-\pi}^{\pi}\log|X(e^{j\omega})|d\omega. \tag{12.55b}$$

[2]Although $\hat{x}[n]$ is referred to as the complex cepstrum it is real valued since $x(e^{j\omega})$ is defined in Eq. (12.53) is conjugate symmetric.

Although it is not at all obvious at this point, in Problem 12.35 and in Chapter 13 we develop the fact that the minimum-phase condition defined in Section 5.6, namely, that $X(z)$ have all its poles and zeros inside the unit circle, guarantees causality of the complex cepstrum. Thus, the minimum-phase condition in Section 5.6 and the condition of causality of the complex cepstrum turn out to be the same constraint developed from different perspectives. Note that when $\hat{x}[n]$ is causal, $\arg[X(e^{j\omega})]$ is completely determined through Eq. (12.54) by $\log|X(e^{j\omega})|$; however, the complete determination of $\log|X(e^{j\omega})|$ by Eq. (12.55a) requires both $\arg[X(e^{j\omega})]$ and the quantity $\hat{x}[0]$. If $\hat{x}[0]$ is not known, then $\log|X(e^{j\omega})|$ is determined only to within an additive constant, or equivalently, $|X(e^{j\omega})|$ is determined only to within a multiplicative (gain) constant.

Minimum phase and causality of the complex cepstrum are not the only constraints that provide a unique relationship between the magnitude and phase of the DTFT. As one example of another type of constraint, it has been shown (Hayes, Lim and Oppenheim, 1980) that if a sequence is of finite length and if its z-transform has no zeros in conjugate reciprocal pairs, then, to within a scale factor, the sequence (and consequently, also the magnitude of the DTFT) is uniquely determined by the phase of the Fourier transform.

12.4 HILBERT TRANSFORM RELATIONS FOR COMPLEX SEQUENCES

Thus far, we have considered Hilbert transform relations for the Fourier transform of causal sequences and the DFT of periodic sequences that are "periodically causal" in the sense that they are zero in the second half of each period. In this section, we consider *complex sequences* for which the real and imaginary components can be related through a discrete convolution similar to the Hilbert transform relations derived in the previous sections. These relations are particularly useful in representing bandpass signals as complex signals in a manner completely analogous to the analytic signals of continuous-time signal theory (Papoulis, 1977).

As mentioned previously, it is possible to base the derivation of the Hilbert transform relations on a notion of causality or one-sidedness. Since we are interested in relating the real and imaginary parts of a complex sequence, one-sidedness will be applied to the DTFT of the sequence. We cannot, of course, require that the DTFT be zero for $\omega < 0$, since it must be periodic. Instead, we consider sequences for which the Fourier transform is zero in the second half of each period; i.e., the z-transform is zero on the bottom half ($-\pi \le \omega < 0$) of the unit circle. Thus, with $x[n]$ denoting the sequence and $X(e^{j\omega})$ its Fourier transform, we require that

$$X(e^{j\omega}) = 0, \qquad -\pi \le \omega < 0. \tag{12.56}$$

(We could just as well assume that $X(e^{j\omega})$ is zero for $0 < \omega \le \pi$.) The sequence $x[n]$ corresponding to $X(e^{j\omega})$ must be complex, since, if $x[n]$ were real, $X(e^{j\omega})$ would be conjugate symmetric, i.e., $X(e^{j\omega}) = X^*(e^{-j\omega})$. Therefore, we express $x[n]$ as

$$x[n] = x_r[n] + jx_i[n], \tag{12.57}$$

where $x_r[n]$ and $x_i[n]$ are real sequences. In continuous-time signal theory, the comparable signal is an analytic function and thus is called an *analytic signal*. Although analyticity has no formal meaning for sequences, we will nevertheless apply the same terminology to complex sequences whose Fourier transforms are one-sided.

If $X_r(e^{j\omega})$ and $X_i(e^{j\omega})$ denote the Fourier transforms of the real sequences $x_r[n]$ and $x_i[n]$, respectively, then

$$X(e^{j\omega}) = X_r(e^{j\omega}) + jX_i(e^{j\omega}), \tag{12.58a}$$

and it follows that

$$X_r(e^{j\omega}) = \frac{1}{2}[X(e^{j\omega}) + X^*(e^{-j\omega})], \tag{12.58b}$$

and

$$jX_i(e^{j\omega}) = \frac{1}{2}[X(e^{j\omega}) - X^*(e^{-j\omega})]. \tag{12.58c}$$

Note that Eq. (12.58c) gives an expression for $jX_i(e^{j\omega})$, which is the Fourier transform of the imaginary signal $jx_i[n]$. Note also that $X_r(e^{j\omega})$ and $X_i(e^{j\omega})$, the Fourier transforms of the real and imaginary parts, respectively, of $x[n]$ are both complex-valued functions. In general, the complex transforms $X_r(e^{j\omega})$ and $jX_i(e^{j\omega})$ play a role similar to that played in the previous sections by the even and odd parts, respectively, of causal sequences. However, $X_r(e^{j\omega})$ is conjugate symmetric, i.e., $X_r(e^{j\omega}) = X_r^*(e^{-j\omega})$. Similarly, $jX_i(e^{j\omega})$ is conjugate antisymmetric, i.e., $jX_i(e^{j\omega}) = -jX_i^*(e^{-j\omega})$.

Figure 12.4 depicts an example of a complex one-sided Fourier transform of a complex sequence $x[n] = x_r[n] + jx_i[n]$, and the corresponding two-sided transforms of the real sequences $x_r[n]$ and $x_i[n]$. This figure shows pictorially the cancellation implied by Eqs. (12.58).

If $X(e^{j\omega})$ is zero for $-\pi \le \omega < 0$, then there is no overlap between the nonzero portions of $X(e^{j\omega})$ and $X^*(e^{-j\omega})$ except at $\omega = 0$. Thus, $X(e^{j\omega})$ can be recovered except at $\omega = 0$ from either $X_r(e^{j\omega})$ or $X_i(e^{j\omega})$. Since $X(e^{j\omega})$ is assumed to be zero at $\omega = \pm\pi$, $X(e^{j\omega})$ is totally recoverable except at $\omega = 0$ from $jX_i(e^{j\omega})$. This is in contrast to the situation in Section 12.2, in which the causal sequence could be recovered from its odd part, except at the endpoints.

In particular,

$$X(e^{j\omega}) = \begin{cases} 2X_r(e^{j\omega}), & 0 < \omega < \pi, \\ 0, & -\pi \le \omega < 0, \end{cases} \tag{12.59}$$

and

$$X(e^{j\omega}) = \begin{cases} 2jX_i(e^{j\omega}), & 0 < \omega < \pi, \\ 0, & -\pi \le \omega < 0. \end{cases} \tag{12.60}$$

Alternatively, we can relate $X_r(e^{j\omega})$ and $X_i(e^{j\omega})$ directly by

$$X_i(e^{j\omega}) = \begin{cases} -jX_r(e^{j\omega}), & 0 < \omega < \pi, \\ jX_r(e^{j\omega}), & -\pi \le \omega < 0, \end{cases} \tag{12.61}$$

or

$$X_i(e^{j\omega}) = H(e^{j\omega})X_r(e^{j\omega}), \tag{12.62a}$$

where

$$H(e^{j\omega}) = \begin{cases} -j, & 0 < \omega < \pi, \\ j, & -\pi < \omega < 0. \end{cases} \tag{12.62b}$$

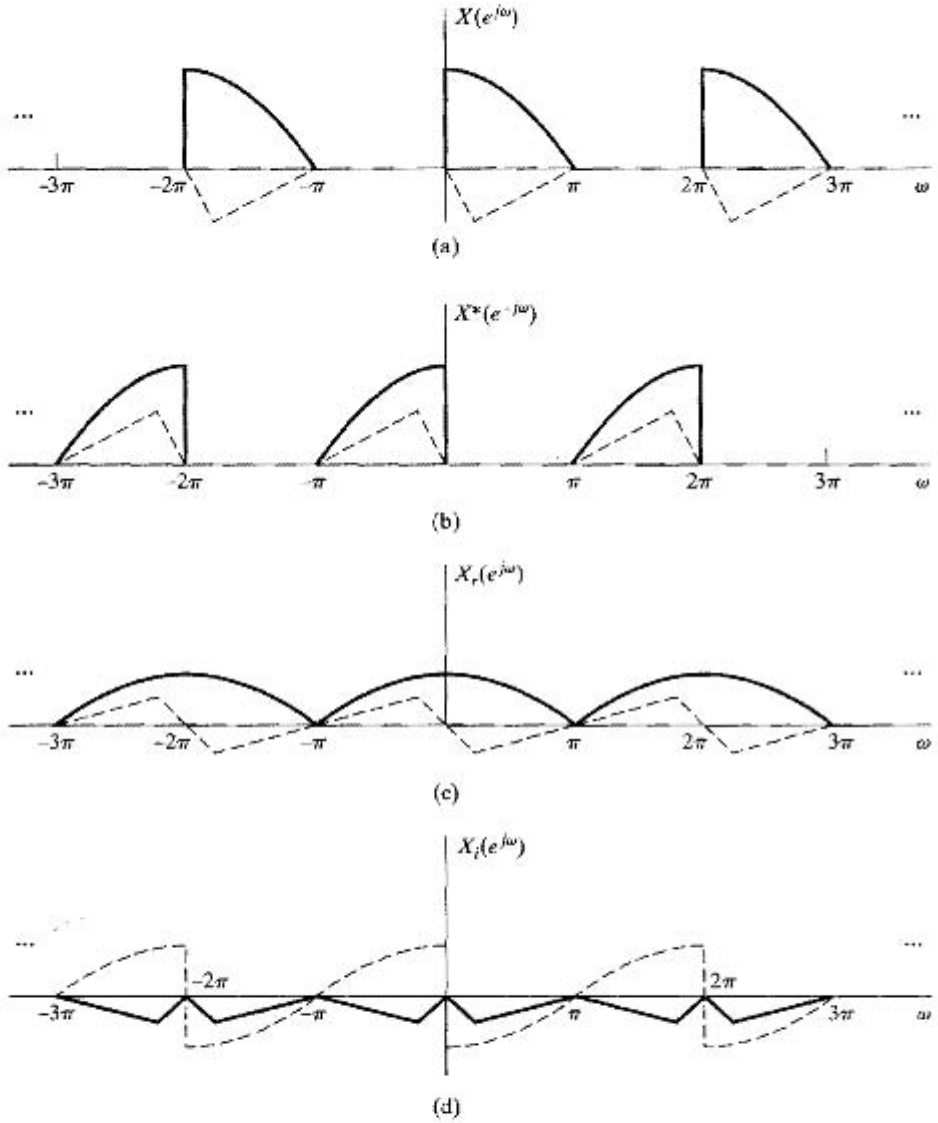

Figure 12.4 Illustration of decomposition of a one-sided Fourier transform. (Solid curves are real parts and dashed curves are imaginary parts.)

Equations (12.62) are illustrated by comparing Figures 12.4(c) and 12.4(d). $X_i(e^{j\omega})$ is the Fourier transform of $x_i[n]$, the imaginary part of $x[n]$, and $X_r(e^{j\omega})$ is the Fourier transform of $x_r[n]$, the real part of $x[n]$. Thus, according to Eqs. (12.62), $x_i[n]$ can be obtained by processing $x_r[n]$ with an LTI discrete-time system with frequency response $H(e^{j\omega})$, as given by Eq. (12.62b). This frequency response has unity magnitude, a phase angle of $-\pi/2$ for $0 < \omega < \pi$, and a phase angle of $+\pi/2$ for $-\pi < \omega < 0$. Such a system is called an ideal 90-degree phase shifter or a *Hilbert transformer*. From Eqs. (12.62), it

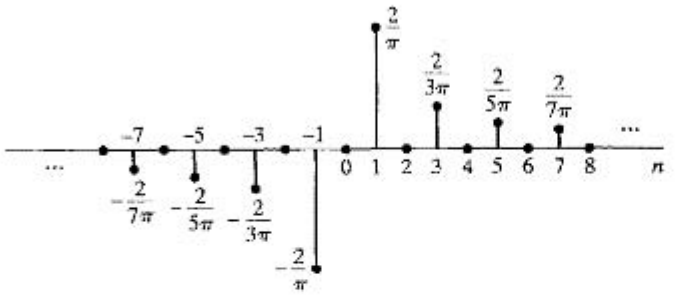

Figure 12.5 Impulse response of an ideal Hilbert transformer or 90-degree phase shifter.

follows that

$$X_r(e^{j\omega}) = \frac{1}{H(e^{j\omega})} X_i(e^{j\omega}) = -H(e^{j\omega}) X_i(e^{j\omega}). \tag{12.63}$$

Thus, $-x_r[n]$ can also be obtained from $x_i[n]$ with a 90-degree phase shifter.

The impulse response $h[n]$ of a 90-degree phase shifter, corresponding to the frequency response $H(e^{j\omega})$ given in Eq. (12.62b), is

$$h[n] = \frac{1}{2\pi} \int_{-\pi}^{0} j e^{j\omega n} d\omega - \frac{1}{2\pi} \int_{0}^{\pi} j e^{j\omega n} d\omega,$$

or

$$h[n] = \begin{cases} \dfrac{2}{\pi} \dfrac{\sin^2(\pi n/2)}{n}, & n \neq 0, \\ 0, & n = 0. \end{cases} \tag{12.64}$$

The impulse response is plotted in Figure 12.5. Using Eqs. (12.62) and (12.63), we obtain the expressions

$$x_i[n] = \sum_{m=-\infty}^{\infty} h[n-m] x_r[m] \tag{12.65a}$$

and

$$x_r[n] = -\sum_{m=-\infty}^{\infty} h[n-m] x_i[m]. \tag{12.65b}$$

Equations (12.65) are the desired Hilbert transform relations between the real and imaginary parts of a discrete-time analytic signal. Figure 12.6 shows how a discrete-time Hilbert transformer system can be used to form a complex analytic signal, which is simply a pair of real signals.

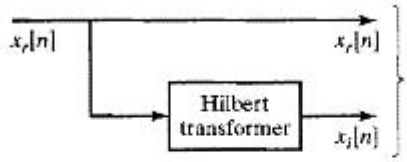

Figure 12.6 Block diagram representation of the creation of a complex sequence whose Fourier transform is one-sided.

12.4.1 Design of Hilbert Transformers

The impulse response of the Hilbert transformer, as given in Eq. (12.64), is not absolutely summable. Consequently,

$$H(e^{j\omega}) = \sum_{n=-\infty}^{\infty} h[n]e^{-j\omega n} \tag{12.66}$$

converges to Eq. (12.62b) only in the mean-square sense. Thus, the ideal Hilbert transformer or 90-degree phase shifter takes its place alongside the ideal lowpass filter and ideal bandlimited differentiator as a valuable theoretical concept that corresponds to a noncausal system and for which the system function exists only in a restricted sense.

Approximations to the ideal Hilbert transformer can, of course, be obtained. FIR approximations with constant group delay can be designed using either the window method or the equiripple approximation method. In such approximations, the 90-degree phase shift is realized exactly, with an additional linear phase component required for a causal FIR system. The properties of these approximations are illustrated by examples of Hilbert transformers designed with Kaiser windows.

Example 12.4 Kaiser Window Design of Hilbert Transformers

The Kaiser window approximation for an FIR discrete Hilbert transformer of order M (length $M+1$) would be of the form

$$h[n] = \begin{cases} \left(\dfrac{I_o[\beta(1-[(n-n_d)/n_d]^2)^{1/2}]}{I_o(\beta)}\right)\left(\dfrac{2}{\pi}\dfrac{\sin^2[\pi(n-n_d)/2]}{n-n_d}\right), & 0 \le n \le M, \\ 0, & \text{otherwise,} \end{cases} \tag{12.67}$$

where $n_d = M/2$. If M is even, the system is a type III FIR generalized linear-phase system, as discussed in Section 5.7.3.

Figure 12.7(a) shows the impulse response, and Figure 12.7(b) shows the magnitude of the frequency response, for $M = 18$ and $\beta = 2.629$. Because $h[n]$ satisfies the symmetry condition $h[n] = -h[M-n]$ for $0 \le n \le M$, the phase is exactly 90 degrees plus a linear-phase component corresponding to a delay of $n_d = 18/2 = 9$ samples; i.e.,

$$\angle H(e^{j\omega}) = \frac{-\pi}{2} - 9\omega, \qquad 0 < \omega < \pi. \tag{12.68}$$

From Figure 12.7(b), we see that, as required for a type III system, the frequency response is zero at $z = 1$ and $z = -1$ ($\omega = 0$ and $\omega = \pi$). Thus, the magnitude response cannot approximate unity very well, except in some middle band $\omega_L < |\omega| < \omega_H$.

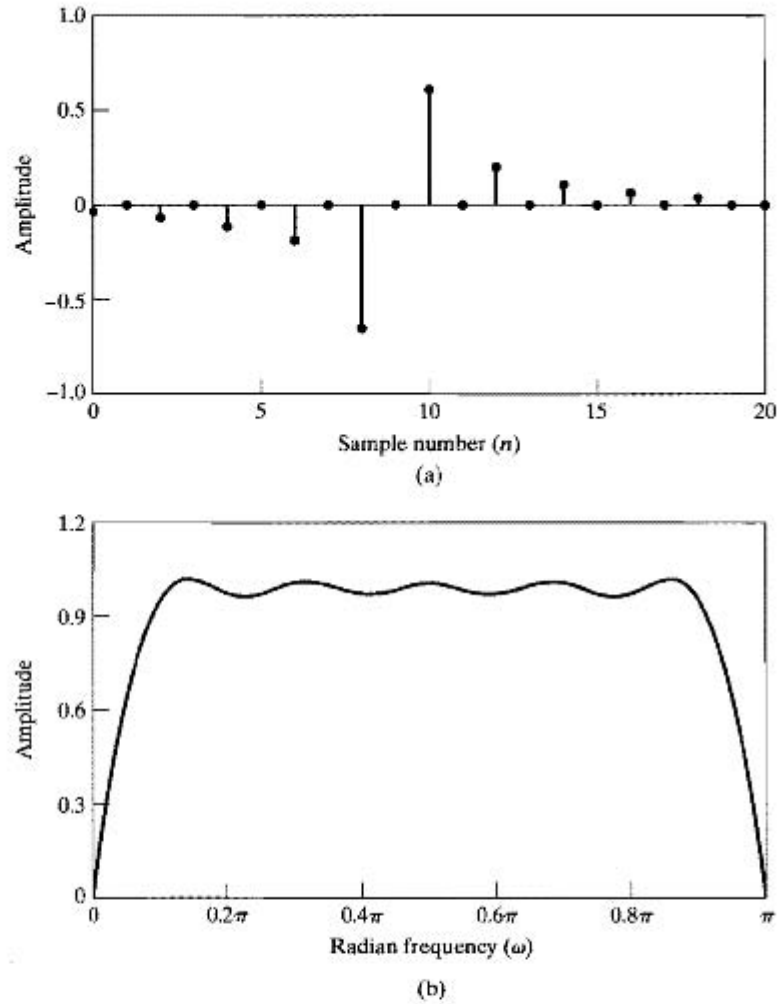

Figure 12.7 (a) Impulse response and (b) magnitude response of an FIR Hilbert transformer designed using the Kaiser window. ($M = 18$ and $\beta = 2.629$.)

If M is an odd integer, we obtain a type IV system, as shown in Figure 12.8, where $M = 17$ and $\beta = 2.44$. For type IV systems, the frequency response is forced to be zero only at $z = 1$ ($\omega = 0$). Therefore, a better approximation to a constant-magnitude response is obtained for frequencies around $\omega = \pi$. The phase response is exactly 90 degrees at all frequencies, plus a linear-phase component corresponding to $n_d = 17/2 = 8.5$ samples delay; i.e.,

$$\angle H(e^{j\omega}) = \frac{-\pi}{2} - 8.5\omega, \qquad 0 < \omega < \pi. \tag{12.69}$$

From a comparison of Figures 12.7(a) and 12.8(a), we see that type III FIR Hilbert transformers have a significant computational advantage over type IV systems when it is not necessary to approximate constant magnitude at $\omega = \pi$. This is because, for type III systems, the even-indexed samples of the impulse response are all exactly zero.

Thus, taking advantage of the antisymmetry in both cases, the system with $M = 17$ would require eight multiplications to compute each output sample, while the system with $M = 18$ would require only five multiplications per output sample.

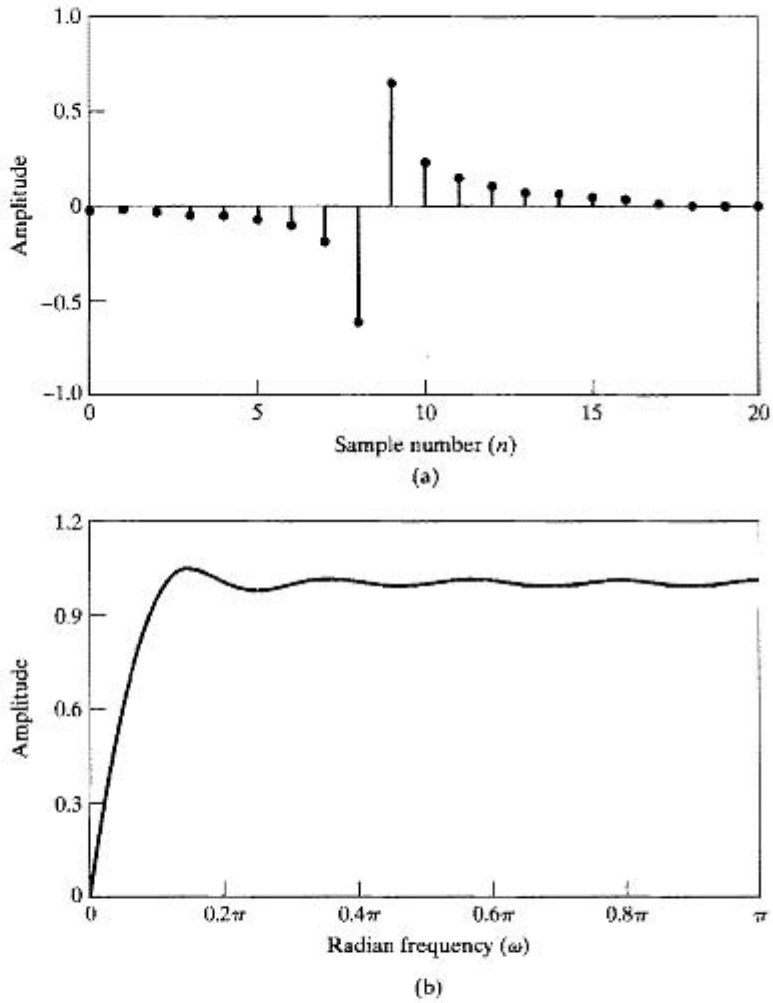

Figure 12.8 (a) Impulse response and (b) magnitude response of an FIR Hilbert transformer designed using the Kaiser window. ($M = 17$ and $\beta = 2.44$.)

Type III and IV FIR linear-phase Hilbert transformer approximations with equiripple magnitude approximation and exactly 90-degree phase can be designed using the Parks–McClellan algorithm as described in Sections 7.7 and 7.8, with the expected improvements in magnitude approximation error over window-designed filters of the same length (see Rabiner and Schafer, 1974).

The exactness of the phase of type III and IV FIR systems is a compelling motivation for their use in approximating Hilbert transformers. IIR systems must have some

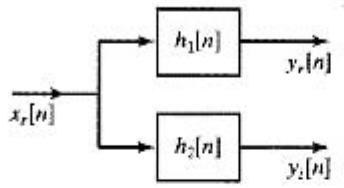

Figure 12.9 Block diagram representation of the allpass phase splitter method for the creation of a complex sequence whose Fourier transform is one-sided.

phase response error as well as magnitude response error in approximating a Hilbert transformer. The most successful approach to designing IIR Hilbert transformers is to design a "phase splitter," which consists of two allpass systems whose phase responses differ by approximately 90 degrees over some portion of the band $0 < |\omega| < \pi$. Such systems can be designed by using the bilinear transformation to transform a continuous-time phase-splitting system to a discrete-time system. (For an example of such a system, see Gold, Oppenheim and Rader, 1970.)

Figure 12.9 depicts a 90-degree phase-splitting system. If $x_r[n]$ denotes a real input signal and $x_i[n]$ its Hilbert transform, then the complex sequence $x[n] = x_r[n] + jx_i[n]$ has a Fourier transform that is identically zero for $-\pi \leq \omega < 0$; i.e., $X(z)$ is zero on the bottom half of the unit circle of the z-plane. In the system of Figure 12.6, a Hilbert transformer was used to form the signal $x_i[n]$ from $x_r[n]$. In Figure 12.9, we process $x_r[n]$ through two systems: $H_1(e^{j\omega})$ and $H_2(e^{j\omega})$. Now, if $H_1(e^{j\omega})$ and $H_2(e^{j\omega})$ are allpass systems whose phase responses differ by 90 degrees, then the complex signal $y[n] = y_r[n] + jy_i[n]$ has a Fourier transform that also vanishes for $-\pi \leq \omega < 0$. Furthermore, $|Y(e^{j\omega})| = |X(e^{j\omega})|$, since the phase-splitting systems are allpass systems. The phases of $Y(e^{j\omega})$ and $X(e^{j\omega})$ will differ by the phase component common to $H_1(e^{j\omega})$ and $H_2(e^{j\omega})$.

12.4.2 Representation of Bandpass Signals

Many of the applications of analytic signals concern narrowband communication. In such applications, it is sometimes convenient to represent a bandpass signal in terms of a lowpass signal. To see how this may be done, consider the complex lowpass signal

$$x[n] = x_r[n] + jx_i[n],$$

where $x_i[n]$ is the Hilbert transform of $x_r[n]$ and

$$X(e^{j\omega}) = 0, \qquad -\pi \leq \omega < 0.$$

The Fourier transforms $X_r(e^{j\omega})$ and $jX_i(e^{j\omega})$ are depicted in Figures 12.10(a) and 12.10(b), respectively, and the resulting transform $X(e^{j\omega}) = X_r(e^{j\omega}) + jX_i(e^{j\omega})$ is shown in Figure 12.10(c). (Solid curves are real parts and dashed curves are imaginary parts.) Now, consider the sequence

$$s[n] = x[n]e^{j\omega_c n} = s_r[n] + js_i[n], \tag{12.70}$$

where $s_r[n]$ and $s_i[n]$ are real sequences. The corresponding Fourier transform is

$$S(e^{j\omega}) = X(e^{j(\omega-\omega_c)}), \tag{12.71}$$

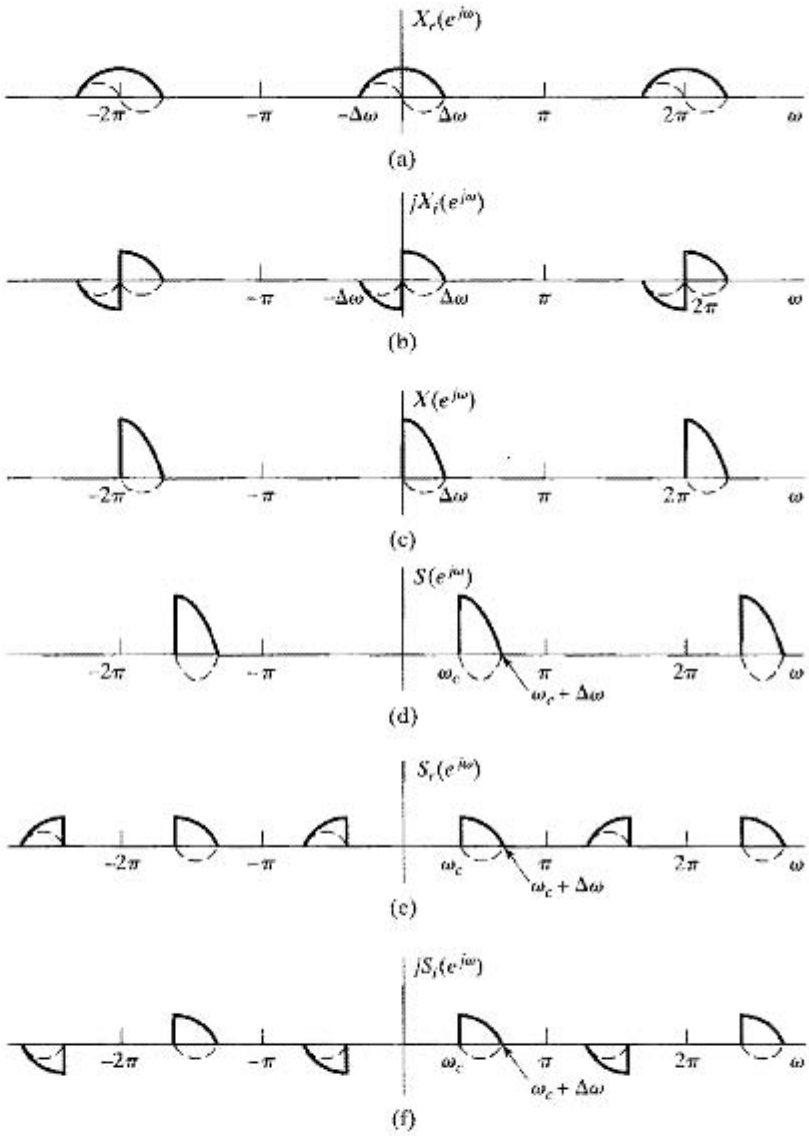

Figure 12.10 Fourier transforms for representation of bandpass signals. (Solid curves are real parts and dashed curves are imaginary parts.) (Note that in parts (b) and (f) the functions $jX_i(e^{j\omega})$ and $jS_i(e^{j\omega})$ are plotted, where $X_i(e^{j\omega})$ and $S_i(e^{j\omega})$ are the Fourier transforms of $x_i[n]$ and $s_i[n]$, respectively.)

which is depicted in Figure 12.10(d). Applying Eqs. (12.58) to $S(e^{j\omega})$ leads to the equations

$$S_r(e^{j\omega}) = \tfrac{1}{2}[S(e^{j\omega}) + S^*(e^{-j\omega})], \tag{12.72a}$$

$$jS_i(e^{j\omega}) = \tfrac{1}{2}[S(e^{j\omega}) - S^*(e^{-j\omega})]. \tag{12.72b}$$

For the example of Figure 12.10, $S_r(e^{j\omega})$ and $jS_i(e^{j\omega})$ are illustrated in Figures 12.10(e) and 12.10(f), respectively. It is straightforward to show that if $X_r(e^{j\omega}) = 0$ for $\Delta\omega < |\omega| \leq \pi$, and if $\omega_c + \Delta\omega < \pi$, then $S(e^{j\omega})$ will be a one-sided bandpass signal such that $S(e^{j\omega}) = 0$ *except* in the interval $\omega_c < \omega \leq \omega_c + \Delta\omega$. As the example of Figure 12.10 illustrates, and as can be shown using Eqs. (12.57) and (12.58), $S_i(e^{j\omega}) = H(e^{j\omega})S_r(e^{j\omega})$, i.e., $s_i[n]$ is the Hilbert transform of $s_r[n]$.

An alternative representation of a complex signal is in terms of magnitude and phase; i.e., $x[n]$ can be expressed as

$$x[n] = A[n]e^{j\phi[n]}, \tag{12.73a}$$

where

$$A[n] = (x_r^2[n] + x_i^2[n])^{1/2} \tag{12.73b}$$

and

$$\phi[n] = \arctan\left(\frac{x_i[n]}{x_r[n]}\right). \tag{12.73c}$$

Therefore, from Eqs. (12.70) and (12.73), we can express $s[n]$ as

$$s[n] = (x_r[n] + jx_i[n])e^{j\omega_c n} \tag{12.74a}$$

$$= A[n]e^{j(\omega_c n + \phi[n])}, \tag{12.74b}$$

from which we obtain the expressions

$$s_r[n] = x_r[n]\cos\omega_c n - x_i[n]\sin\omega_c n, \tag{12.75a}$$

or

$$s_r[n] = A[n]\cos(\omega_c n + \phi[n]), \tag{12.75b}$$

and

$$s_i[n] = x_r[n]\sin\omega_c n + x_i[n]\cos\omega_c n, \tag{12.76a}$$

or

$$s_i[n] = A[n]\sin(\omega_c n + \phi[n]). \tag{12.76b}$$

Equations (12.75a) and (12.76a) are depicted in Figures 12.11(a) and 12.11(b), respectively. These diagrams illustrate how a complex bandpass (single-sideband) signal can be formed from a real lowpass signal.

Taken together, Eqs. (12.75) and (12.76) are the desired time-domain representations of a general complex bandpass signal $s[n]$ in terms of the real and imaginary parts of a complex lowpass signal $x[n]$. Generally, this complex representation is a convenient mechanism for representing a real bandpass signal. For example, Eq. (12.75a) provides a time-domain representation of the real bandpass signal in terms of an "in-phase" component $x_r[n]$ and a "quadrature" (90-degree phase-shifted) component $x_i[n]$. Indeed, as illustrated in Figure 12.10(e), Eq. (12.75a) permits the representation of real bandpass signals (or filter impulse responses) whose Fourier transforms are not conjugate symmetric about the center of the passband (as would be the case for signals of the form $x_r[n]\cos\omega_c n$).

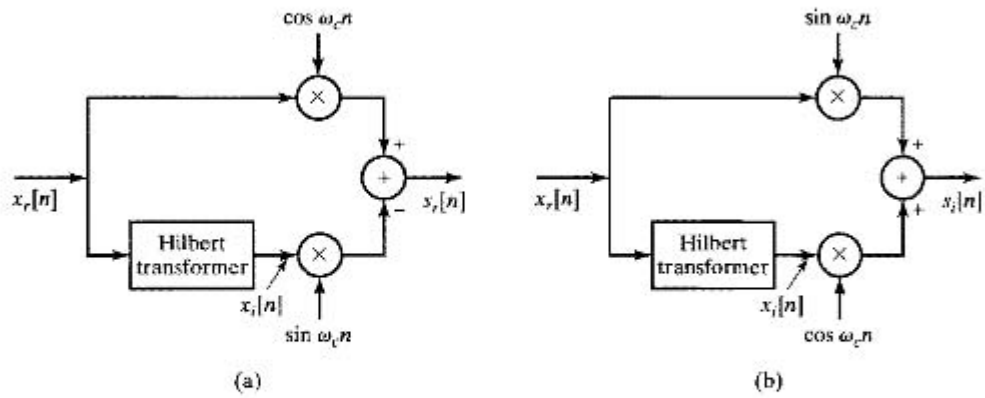

Figure 12.11 Block diagram representation of Eqs. (12.75a) and (12.76a) for obtaining a single-sideband signal.

It is clear from the form of Eqs. (12.75) and (12.76) and from Figure 12.11 that a general bandpass signal has the form of a sinusoid that is both amplitude and phase modulated. The sequence $A[n]$ is called the envelope and $\phi[n]$ the phase. This narrowband signal representation can be used to represent a variety of amplitude and phase modulation systems. The example of Figure 12.10 is an illustration of single-sideband modulation. If we consider the real signal $s_r[n]$ as resulting from single-sideband modulation with the lowpass real signal $x_r[n]$ as the input, then Figure 12.11(a) represents a scheme for implementing the single-sideband modulation system. Single-sideband modulation systems are useful in frequency-division multiplexing, since they can represent a real bandpass signal with minimum bandwidth.

12.4.3 Bandpass Sampling

Another important use of analytic signals is in the sampling of bandpass signals. In Chapter 4, we saw that, in general, if a continuous-time signal has a bandlimited Fourier transform such that $S_c(j\Omega) = 0$ for $|\Omega| \geq \Omega_N$, then the signal is exactly represented by its samples if the sampling rate satisfies the inequality $2\pi/T \geq 2\Omega_N$. The key to the proof of this result is to avoid overlapping the replicas of $S_c(j\Omega)$ that form the DTFT of the sequence of samples. A bandpass continuous-time signal has a Fourier transform such that $S_c(j\Omega) = 0$ for $0 \leq |\Omega| \leq \Omega_c$ and for $|\Omega| \geq \Omega_c + \Delta\Omega$. Thus, its bandwidth, or region of support, is really only $2\Delta\Omega$ rather than $2(\Omega_c + \Delta\Omega)$, and with a proper sampling strategy, the region $-\Omega_c \leq \Omega \leq \Omega_c$ can be filled with images of the nonzero part of $S_c(j\Omega)$ without overlapping. This is greatly facilitated by using a complex representation of the bandpass signal.

As an illustration, consider the system of Figure 12.12 and the signal shown in Figure 12.13(a). The highest frequency of the input signal is $\Omega_c + \Delta\Omega$. If this signal is sampled at exactly the Nyquist rate, $2\pi/T = 2(\Omega_c + \Delta\Omega)$, then the resulting sequence of samples, $s_r[n] = s_c(nT)$, has the Fourier transform $S_r(e^{j\omega})$ plotted in Figure 12.13(b). Using a discrete-time Hilbert transformer, we can form the complex sequence $s[n] = s_r[n] + js_i[n]$ whose Fourier transform is $S(e^{j\omega})$ in Figure 12.13(c). The

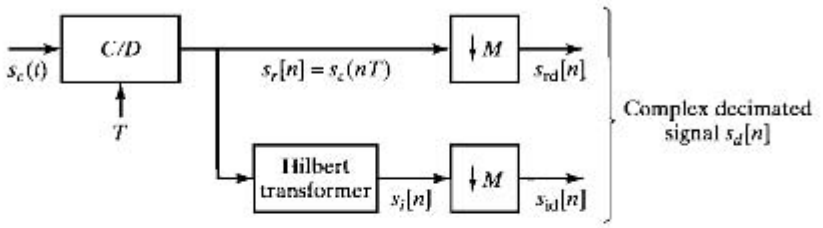

Figure 12.12 System for reduced-rate sampling of a real bandpass signal by decimation of the equivalent complex bandpass signal.

width of the nonzero region of $S(e^{j\omega})$ is $\Delta\omega = (\Delta\Omega)T$. Defining M as the largest integer less than or equal to $2\pi/\Delta\omega$, we see that M copies of $S(e^{j\omega})$ would fit into the interval $-\pi < \omega < \pi$. (In the example of Figure 12.13(c), $2\pi/\Delta\omega = 5$.) Thus, the sampling rate of $s[n]$ can be reduced by decimation as shown in Figure 12.12, yielding the reduced-rate complex sequence $s_d[n] = s_{rd}[n] + js_{id}[n] = s[Mn]$ whose Fourier transform is

$$S_d(e^{j\omega}) = \frac{1}{M}\sum_{k=0}^{M-1} S(e^{j[(\omega-2\pi k)/M]}). \tag{12.77}$$

Figure 12.13(d) shows $S_d(e^{j\omega})$ with $M = 5$ in Eq. (12.77). $S(e^{j\omega})$ and two of the frequency-scaled and translated copies of $S(e^{j\omega})$ are indicated explicitly in Figure 12.13(d). It is clear that aliasing has been avoided and that all the information necessary to reconstruct the original sampled real bandpass signal now resides in the discrete-time frequency interval $-\pi < \omega \leq \pi$. A complex filter applied to $s_d[n]$ can transform this information in useful ways, such as by further bandlimiting, amplitude or phase compensation, etc., or the complex signal can be coded for transmission or digital storage. This processing takes place at the low sampling rate, and this is, of course, the motivation for reducing the sampling rate.

The original real bandpass signal $s_r[n]$ can be reconstructed ideally by the following procedure:

1. Expand the complex sequence by a factor M; i.e., obtain

$$s_e[n] = \begin{cases} s_{rd}[n/M] + js_{id}[n/M], & n = 0, \pm M, \pm 2M, \ldots, \\ 0, & \text{otherwise.} \end{cases} \tag{12.78}$$

2. Filter the signal $s_e[n]$ using an ideal *complex* bandpass filter with impulse response $h_i[n]$ and frequency response

$$H_i(e^{j\omega}) = \begin{cases} 0, & -\pi < \omega < \omega_c, \\ M, & \omega_c < \omega < \omega_c + \Delta\omega, \\ 0, & \omega_c + \Delta\omega < \omega < \pi. \end{cases} \tag{12.79}$$

(In our example, $\omega_c + \Delta\omega = \pi$.)

3. Obtain $s_r[n] = \mathcal{R}e\{s_e[n] * h_i[n]\}$.

A useful exercise is to plot the Fourier transform $S_e(e^{j\omega})$ for the example of Figure 12.13 and verify that the filter of Eq. (12.79) does indeed recover $s[n]$.

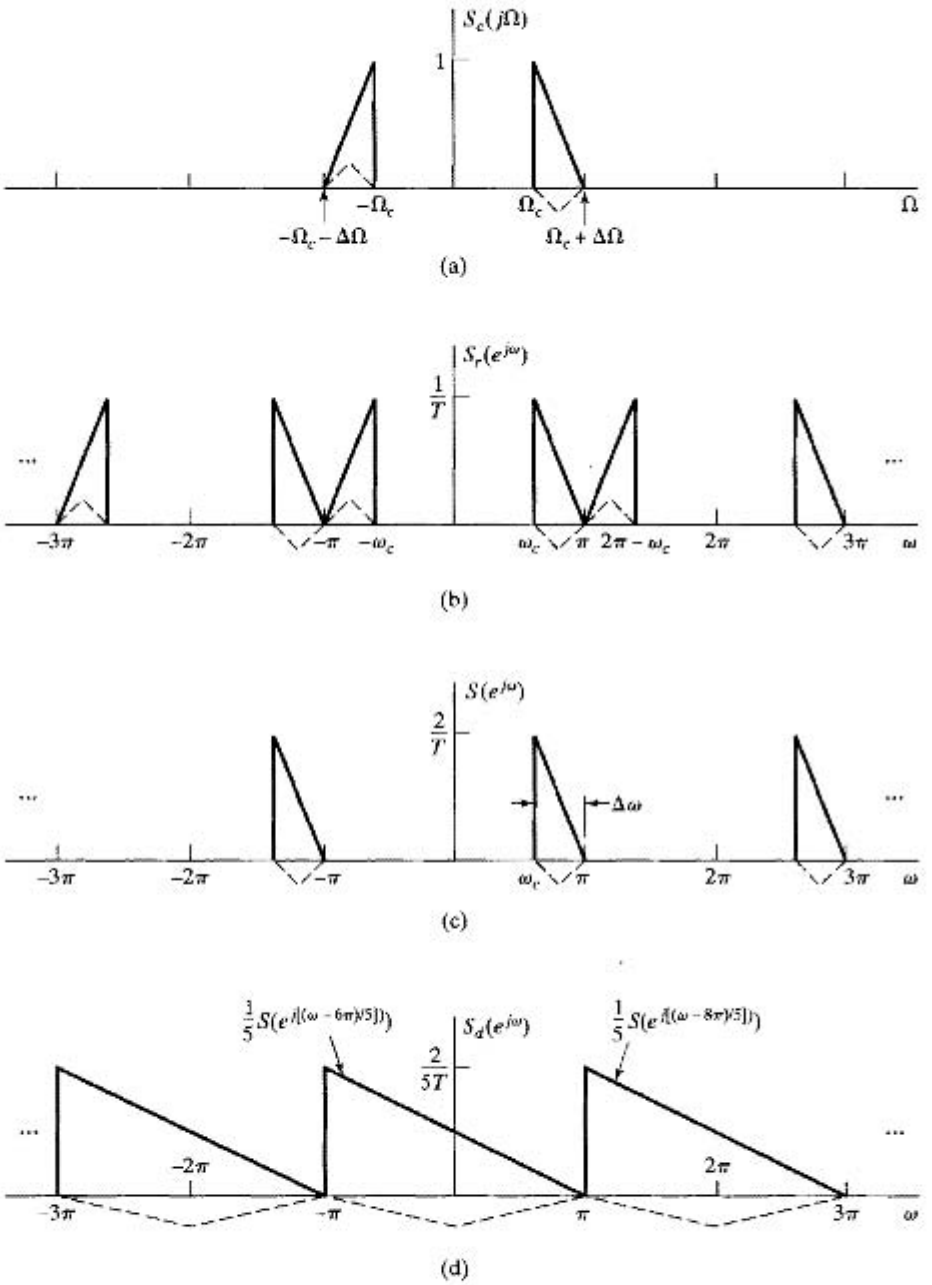

Figure 12.13 Example of reduced-rate sampling of a bandpass signal using the system of Figure 12.12. (a) Fourier transform of continuous-time bandpass signal. (b) Fourier transform of sampled signal. (c) Fourier transform of complex bandpass discrete-time signal derived from the signal of part (a). (d) Fourier transform of decimated complex bandpass of part (c). (Solid curves are real parts and dashed curves are imaginary parts.)

Another useful exercise is to consider a complex continuous-time signal with a one-sided Fourier transform equal to $S_c(j\Omega)$ for $\Omega \geq 0$. It can be shown that such a signal can be sampled with sampling rate $2\pi/T = \Delta\Omega$, directly yielding the complex sequence $s_d[n]$.

12.5 SUMMARY

In this chapter, we have discussed a variety of relations between the real and imaginary parts of Fourier transforms and the real and imaginary parts of complex sequences. These relationships are collectively referred to as *Hilbert transform relationships*. Our approach to deriving all the Hilbert transform relations was to apply a basic causality principle that allows a sequence or function to be recovered from its even part. We showed that, for a causal sequence, the real and imaginary parts of the Fourier transform are related through a convolution-type integral. Also, for the special case when the complex cepstrum of a sequence is causal or, equivalently, both the poles and zeros of its z-transform lie inside the unit circle (the minimum-phase condition), the logarithm of the magnitude and the phase of the Fourier transform are a Hilbert transform pair of each other.

Hilbert transform relations were derived for periodic sequences that satisfy a modified causality constraint and for complex sequences whose Fourier transforms vanish on the bottom half of the unit circle. Applications of complex analytic signals to the representation and efficient sampling of bandpass signals were also discussed.

Problems

Basic Problems

12.1. Consider a sequence $x[n]$ with DTFT $X(e^{j\omega})$. The sequence $x[n]$ is real valued and causal, and

$$\mathcal{R}e\{X(e^{j\omega})\} = 2 - 2a\cos\omega.$$

Determine $\mathcal{I}m\{X(e^{j\omega})\}$.

12.2. Consider a sequence $x[n]$ and its DTFT $X(e^{j\omega})$. The following is known:

$$x[n] \text{ is real and causal,}$$
$$\mathcal{R}e\{X(e^{j\omega})\} = \tfrac{5}{4} - \cos\omega.$$

Determine a sequence $x[n]$ consistent with the given information.

12.3. Consider a sequence $x[n]$ and its DTFT $X(e^{j\omega})$. The following is known:

$$x[n] \text{ is real,}$$
$$x[0] = 0,$$
$$x[1] > 0,$$
$$|X(e^{j\omega})|^2 = \tfrac{5}{4} - \cos\omega.$$

Determine two distinct sequences $x_1[n]$ and $x_2[n]$ consistent with the given information.

12.4. Consider a complex sequence $x[n] = x_r[n] + jx_i[n]$, where $x_r[n]$ and $x_i[n]$ are the real part and imaginary part, respectively. The z-transform $X(z)$ of the sequence $x[n]$ is zero on the bottom half of the unit circle; i.e., $X(e^{j\omega}) = 0$ for $\pi \leq \omega < 2\pi$. The real part of $x[n]$ is

$$x_r[n] = \begin{cases} 1/2, & n = 0, \\ -1/4, & n = \pm 2, \\ 0, & \text{otherwise.} \end{cases}$$

Determine the real and imaginary parts of $X(e^{j\omega})$.

12.5. Find the Hilbert transforms $x_i[n] = \mathcal{H}\{x_r[n]\}$ of the following sequences:

(a) $x_r[n] = \cos \omega_0 n$
(b) $x_r[n] = \sin \omega_0 n$
(c) $x_r[n] = \dfrac{\sin(\omega_0 n)}{\pi n}$

12.6. The imaginary part of $X(e^{j\omega})$ for a causal, real sequence $x[n]$ is

$$X_I(e^{j\omega}) = 2 \sin \omega - 3 \sin 4\omega.$$

Additionally, it is known that $X(e^{j\omega})|_{\omega=0} = 6$. Find $x[n]$.

12.7. **(a)** $x[n]$ is a real, causal sequence with the imaginary part of its DTFT $X(e^{j\omega})$ given by

$$\mathcal{I}m\{X(e^{j\omega})\} = \sin \omega + 2 \sin 2\omega.$$

Determine a choice for $x[n]$.

(b) Is your answer to part (a) unique? If so, explain why. If not, determine a second, distinct choice for $x[n]$ satisfying the relationship given in part (a).

12.8. Consider a real, causal sequence $x[n]$ with DTFT $X(e^{j\omega}) = X_R(e^{j\omega}) + jX_I(e^{j\omega})$. The imaginary part of the DTFT is

$$X_I(e^{j\omega}) = 3 \sin(2\omega).$$

Which of the real parts $X_{Rm}(e^{j\omega})$ listed below are consistent with this information:

$$X_{R1}(e^{j\omega}) = \frac{3}{2} \cos(2\omega),$$
$$X_{R2}(e^{j\omega}) = -3 \cos(2\omega) - 1,$$
$$X_{R3}(e^{j\omega}) = -3 \cos(2\omega),$$
$$X_{R4}(e^{j\omega}) = 2 \cos(3\omega),$$
$$X_{R5}(e^{j\omega}) = \frac{3}{2} \cos(2\omega) + 1.$$

12.9. The following information is known about a real, causal sequence $x[n]$ and its DTFT $X(e^{j\omega})$:

$$\mathcal{I}m\{X(e^{j\omega})\} = 3\sin(\omega) + \sin(3\omega),$$
$$X(e^{j\omega})|_{\omega=\pi} = 3.$$

Determine a sequence $x[n]$ consistent with this information. Is the sequence unique?

12.10. Consider $h[n]$, the real-valued impulse response of a stable, causal LTI system with frequency response $H(e^{j\omega})$. The following is known:

(i) The system has a stable, causal inverse.

(ii) $\left|H(e^{j\omega})\right|^2 = \dfrac{\frac{5}{4} - \cos\omega}{5 + 4\cos\omega}$.

Determine $h[n]$ in as much detail as possible.

12.11. Let $x[n] = x_r[n] + jx_i[n]$ be a complex-valued sequence such that $X(e^{j\omega}) = 0$ for $-\pi \leq \omega < 0$. The imaginary part is

$$x_I[n] = \begin{cases} 4, & n = 3, \\ -4, & n = -3. \end{cases}$$

Specify the real and imaginary parts of $X(e^{j\omega})$.

12.12. $h[n]$ is a causal, real-valued sequence with $h[0]$ nonzero and positive. The magnitude squared of the frequency response of $h[n]$ is given by

$$\left|H(e^{j\omega})\right|^2 = \frac{10}{9} - \frac{2}{3}\cos(\omega).$$

(a) Determine a choice for $h[n]$.

(b) Is your answer to part (b) unique? If so, explain why. If not, determine a second, distinct choice for $h[n]$ satisfying the given conditions.

12.13. Let $x[n]$ denote a causal, complex-valued sequence with Fourier transform

$$X(e^{j\omega}) = X_R(e^{j\omega}) + jX_I(e^{j\omega}).$$

If $X_R(e^{j\omega}) = 1 + \cos(\omega) + \sin(\omega) - \sin(2\omega)$, determine $X_I(e^{j\omega})$.

12.14. Consider a real, anticausal sequence $x[n]$ with DTFT $X(e^{j\omega})$. The real part of $X(e^{j\omega})$ is

$$X_R(e^{j\omega}) = \sum_{k=0}^{\infty} (1/2)^k \cos(k\omega).$$

Find $X_I(e^{j\omega})$, the imaginary part of $X(e^{j\omega})$. (Remember that a sequence is said to be anticausal if $x[n] = 0$ for $n > 0$.)

12.15. $x[n]$ is a real, causal sequence with DTFT $X(e^{j\omega})$. The imaginary part of $X(e^{j\omega})$ is

$$\mathcal{I}m\{X(e^{j\omega})\} = \sin\omega,$$

and it is also known that

$$\sum_{n=-\infty}^{\infty} x[n] = 3.$$

Determine $x[n]$.

12.16. Consider a real, causal sequence $x[n]$ with DTFT $X(e^{j\omega})$, where the following two facts are given about $X(e^{j\omega})$:

$$X_R(e^{j\omega}) = 2 - 4\cos(3\omega),$$

$$X(e^{j\omega})|_{\omega=\pi} = 7.$$

Are these facts consistent? That is, can a sequence $x[n]$ satisfy both? If so, give one choice for $x[n]$. If not, explain why not.

12.17. Consider a real, causal, finite-length signal $x[n]$ with length $N = 2$ and with a 2-point DFT $X[k] = X_R[k] + jX_I[k]$ for $k = 0, 1$. If $X_R[k] = 2\delta[k] - 4\delta[k-1]$, is it possible to determine $x[n]$ uniquely? If so, give $x[n]$. If not, give several choices for $x[n]$ satisfying the stated condition on $X_R[k]$.

12.18. Let $x[n]$ be a real-valued, causal, finite-length sequence with length $N = 3$. Find two choices for $x[n]$ such that the real part of the DFT $X_R[k]$ matches that shown in Figure P12.18. Note that only one of your sequences is "periodically causal" according to the definition in Section 10.2, where $x[n] = 0$ for $N/2 < n \leq N-1$.

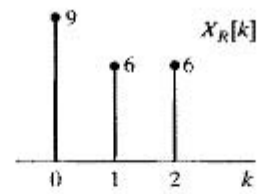

Figure P12.18

12.19. Let $x[n]$ be a real, causal, finite-length sequence with length $N = 4$ that is also periodically causal. The real part of the 4-point DFT $X_R[k]$ for this sequence is shown in Figure P12.19. Determine the imaginary part of the DFT $jX_I[k]$.

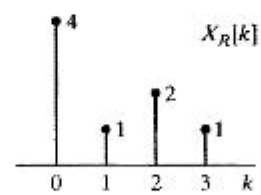

Figure P12.19

12.20. Consider a sequence $x[n]$ that is real, causal, and of finite length with $N = 6$. The imaginary part of the 6-point DFT of this sequence is

$$jX_I[k] = \begin{cases} -j2/\sqrt{3}, & k = 2, \\ j2/\sqrt{3}, & k = 4, \\ 0, & \text{otherwise.} \end{cases}$$

Additionally, it is known that

$$\frac{1}{6}\sum_{k=0}^{5} X[k] = 1.$$

Which of the sequences shown in Figure P12.20 are consistent with the information given?

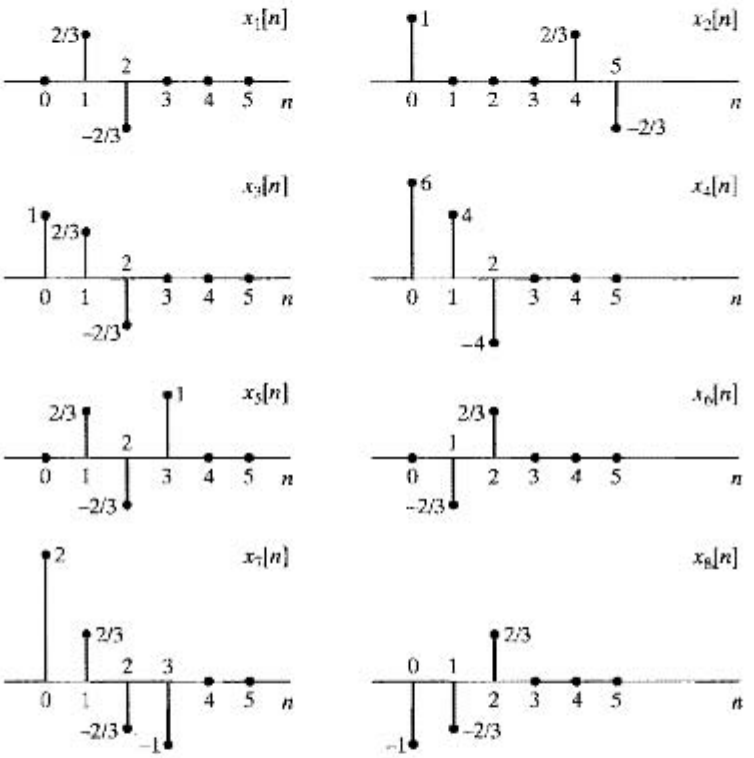

Figure P12.20

12.21. Let $x[n]$ be a real causal sequence for which $|x[n]| < \infty$. The z-transform of $x[n]$ is

$$X(z) = \sum_{n=0}^{\infty} x[n]z^{-n},$$

which is a Taylor's series in the variable z^{-1} and therefore converges to an analytic function everywhere outside some circular disc centered at $z = 0$. (The ROC includes the point $z = \infty$, and, in fact, $X(\infty) = x[0]$.) The statement that $X(z)$ is analytic (in its ROC) implies strong constraints on the function $X(z)$. (See Churchill and Brown, 1990.) Specifically, its real and imaginary parts each satisfy Laplace's equation, and the real and imaginary parts are related by the Cauchy–Riemann equations. We will use these properties to determine $X(z)$ from its real part when $x[n]$ is a real, finite-valued, causal sequence.

Let the z-transform of such a sequence be

$$X(z) = X_R(z) + jX_I(z).$$

where $X_R(z)$ and $X_I(z)$ are real-valued functions of z. Suppose that $X_R(z)$ is

$$X_R(\rho e^{j\omega}) = \frac{\rho + \alpha\cos\omega}{\rho}, \qquad \alpha \text{ real},$$

for $z = \rho e^{j\omega}$. Then find $X(z)$ (as an explicit function of z), assuming that $X(z)$ is analytic everywhere except at $z = 0$. Do this using both of the following methods.

(a) *Method 1, Frequency Domain.* Use the fact that the real and imaginary parts of $X(z)$ must satisfy the Cauchy–Riemann equations everywhere that $X(z)$ is analytic. The Cauchy–Riemann equations are the following:

1. In Cartesian coordinates,

$$\frac{\partial U}{\partial x} = \frac{\partial V}{\partial y}, \qquad \frac{\partial V}{\partial x} = -\frac{\partial U}{\partial y},$$

where $z = x + jy$ and $X(x + jy) = U(x, y) + jV(x, y)$.

2. In polar coordinates,

$$\frac{\partial U}{\partial \rho} = \frac{1}{\rho}\frac{\partial V}{\partial \omega}, \qquad \frac{\partial V}{\partial \rho} = -\frac{1}{\rho}\frac{\partial U}{\partial \omega},$$

where $z = \rho e^{j\omega}$ and $X(\rho e^{j\omega}) = U(\rho, \omega) + jV(\rho, \omega)$.

Since we know that $U = X_R$, we can integrate these equations to find $V = X_I$ and hence X. (Be careful to treat the constant of integration properly.)

(b) *Method 2, Time Domain.* The sequence $x[n]$ can be represented as $x[n] = x_e[n] + x_o[n]$, where $x_e[n]$ is real and even with Fourier transform $X_R(e^{j\omega})$ and the sequence $x_o[n]$ is real and odd with Fourier transform $jX_I(e^{j\omega})$. Find $x_e[n]$ and, using causality, find $x_o[n]$ and hence $x[n]$ and $X(z)$.

12.22. $x[n]$ is a causal, real-valued sequence with Fourier transform $X(e^{j\omega})$. It is known that

$$\mathrm{Re}\{X(e^{j\omega})\} = 1 + 3\cos\omega + \cos 3\omega.$$

Determine a choice for $x[n]$ consistent with this information, and specify whether or not your choice is unique.

12.23. $x[n]$ is a real-valued, causal sequence with DTFT $X(e^{j\omega})$. Determine a choice for $x[n]$ if the imaginary part of $X(e^{j\omega})$ is given by:

$$\mathrm{Im}\{X(e^{j\omega})\} = 3\sin(2\omega) - 2\sin(3\omega).$$

12.24. Show that the sequence of DFS coefficients for the sequence

$$\tilde{u}_N[n] = \begin{cases} 1, & n = 0, \quad N/2, \\ 2, & n = 1, 2, \ldots, N/2 - 1, \\ 0, & n = N/2 + 1, \ldots, N - 1, \end{cases}$$

is

$$\tilde{U}_N[k] = \begin{cases} N, & k = 0, \\ -j2\cot(\pi k/N), & k \text{ odd}, \\ 0, & k \text{ even}, k \neq 0. \end{cases}$$

Hint: Find the z-transform of the sequence

$$u_N[n] = 2u[n] - 2u[n - N/2] - \delta[n] + \delta[n - N/2],$$

and sample it to obtain $\tilde{U}[k]$.

Advanced Problems

12.25. Consider a real-valued finite-duration sequence $x[n]$ of length M. Specifically, $x[n] = 0$ for $n < 0$ and $n > M - 1$. Let $X[k]$ denote the N-point DFT of $x[n]$ with $N \geq M$ and N odd. The real part of $X[k]$ is denoted $X_R[k]$.

(a) Determine, in terms of M, the smallest value of N that will permit $X[k]$ to be uniquely determined from $X_R[k]$.

(b) With N satisfying the condition determined in part (a), $X[k]$ can be expressed as the circular convolution of $X_R[k]$ with a sequence $U_N[k]$. Determine $U_N[k]$.

12.26. $y_r[n]$ is a real-valued sequence with DTFT $Y_r(e^{j\omega})$. The sequences $y_r[n]$ and $y_i[n]$ in Figure P12.26 are interpreted as the real and imaginary parts of a complex sequence $y[n]$, i.e., $y[n] = y_r[n] + jy_i[n]$. Determine a choice for $H(e^{j\omega})$ in Figure P12.26 so that $Y(e^{j\omega})$ is $Y_r(e^{j\omega})$ for *negative* frequencies and zero for *positive* frequencies between $-\pi$ and π, i.e.,

$$Y(e^{j\omega}) = \begin{cases} Y_r(e^{j\omega}), & -\pi < \omega < 0 \\ 0, & 0 < \omega < \pi \end{cases}$$

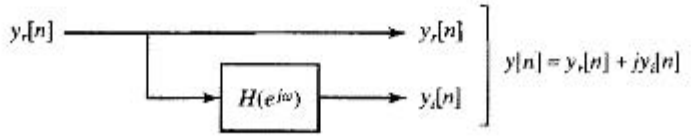

Figure P12.26 System for obtaining $y[n]$ from $y_r[n]$.

12.27. Consider a complex sequence $h[n] = h_r[n] + jh_i[n]$, where $h_r[n]$ and $h_i[n]$ are both real sequences, and let $H(e^{j\omega}) = H_R(e^{j\omega}) + jH_I(e^{j\omega})$ denote the Fourier transform of $h[n]$, where $H_R(e^{j\omega})$ and $H_I(e^{j\omega})$ are the real and imaginary parts, respectively, of $H(e^{j\omega})$.

Let $H_{ER}(e^{j\omega})$ and $H_{OR}(e^{j\omega})$ denote the even and odd parts, respectively, of $H_R(e^{j\omega})$, and let $H_{EI}(e^{j\omega})$, and $H_{OI}(e^{j\omega})$ denote the even and odd parts, respectively, of $H_I(e^{j\omega})$. Furthermore, let $H_A(e^{j\omega})$ and $H_B(e^{j\omega})$ denote the real and imaginary parts of the Fourier transform of $h_r[n]$, and let $H_C(e^{j\omega})$ and $H_D(e^{j\omega})$ denote the real and imaginary parts of the Fourier transform of $h_i[n]$. Express $H_A(e^{j\omega})$, $H_B(e^{j\omega})$, $H_C(e^{j\omega})$, and $H_D(e^{j\omega})$ in terms of $H_{ER}(e^{j\omega})$, $H_{OR}(e^{j\omega})$, $H_{EI}(e^{j\omega})$, and $H_{OI}(e^{j\omega})$.

12.28. The ideal Hilbert transformer (90-degree phase shifter) has frequency response (over one period)

$$H(e^{j\omega}) = \begin{cases} -j, & \omega > 0, \\ j, & \omega < 0. \end{cases}$$

Figure P12.28-1 shows $H(e^{j\omega})$, and Figure P12.28-2 shows the frequency response of an ideal lowpass filter $H_{lp}(e^{j\omega})$ with cutoff frequency $\omega_c = \pi/2$. These frequency responses are clearly similar, each having discontinuities separated by π.

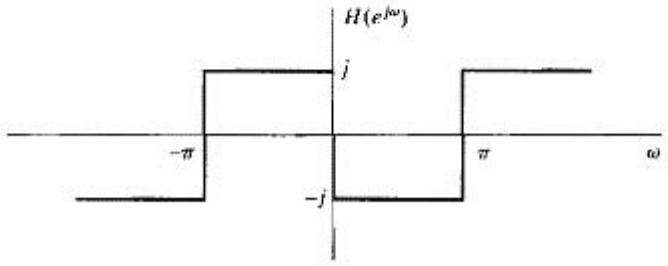

Figure P12.28-1

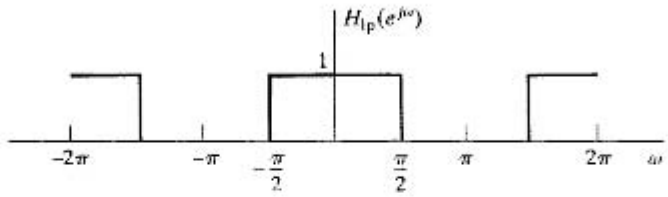

Figure P12.28-2

(a) Obtain a relationship that expresses $H(e^{j\omega})$ in terms of $H_{lp}(e^{j\omega})$. Solve this equation for $H_{lp}(e^{j\omega})$ in terms of $H(e^{j\omega})$.

(b) Use the relationships in part (a) to obtain expressions for $h[n]$ in terms of $h_{lp}[n]$ and for $h_{lp}[n]$ in terms of $h[n]$.

The relationships obtained in parts (a) and (b) were based on definitions of ideal systems with zero phase. However, similar relationships hold for nonideal systems with generalized linear phase.

(c) Use the results of part (b) to obtain a relationship between the impulse response of a causal FIR approximation to the Hilbert transformer and the impulse response of a causal FIR approximation to the lowpass filter, both of which are designed by (1) incorporating an appropriate linear phase, (2) determining the corresponding ideal impulse response, and (3) multiplying by the same window of length $(M+1)$ samples, i.e., by the window method discussed in Chapter 7. (If necessary, consider the cases of M even and M odd separately.)

(d) For the Hilbert transformer approximations of Example 12.4, sketch the magnitude of the frequency responses of the corresponding lowpass filters.

12.29. In Section 12.4.3, we discussed an efficient scheme for sampling a bandpass continuous-time signal with Fourier transform such that

$$S_c(j\Omega) = 0 \qquad \text{for} \quad |\Omega| \le \Omega_c \quad \text{and} \quad |\Omega| \ge \Omega_c + \Delta\Omega.$$

In that discussion, it was assumed that the signal was initially sampled with sampling frequency $2\pi/T = 2(\Omega_c + \Delta\Omega)$. The bandpass sampling scheme is depicted in Figure 12.12. After we form a complex bandpass discrete-time signal $s[n]$ with one-sided Fourier transform $S(e^{j\omega})$, the complex signal is decimated by a factor M, which is assumed to be the largest integer less than or equal to $2\pi/(\Delta\Omega T)$.

(a) By carrying through an example such as the one depicted in Figure 12.13, show that if the quantity $2\pi/(\Delta\Omega T)$ is not an integer for the initial sampling rate chosen, then the resulting decimated signal $s_d[n]$ will have regions of nonzero length where its Fourier transform $S_d(e^{j\omega})$ is identically zero.

(b) How should the initial sampling frequency $2\pi/T$ be chosen so that a decimation factor M can be found such that the decimated sequence $s_d[n]$ in the system of Figure 12.12 will have a Fourier transform $S_d(e^{j\omega})$ that is not aliased yet has no regions where it is zero over an interval of nonzero length?

12.30. Consider an LTI system with frequency response.

$$H(e^{j\omega}) = \begin{cases} 1, & 0 \le \omega \le \pi, \\ 0, & -\pi < \omega < 0. \end{cases}$$

The input $x[n]$ to the system is restricted to be real valued and to have a Fourier transform (i.e., $x[n]$ is absolutely summable). Determine whether or not it is possible to always uniquely recover the system input from the system output. If it is possible, describe how. If it is not possible, explain why not.

Extension Problems

12.31. Derive an integral expression for $H(z)$ *outside* the unit circle in terms of $\mathcal{R}e\{H(e^{j\omega})\}$ when $h[n]$ is a real, stable, and causal sequence, i.e., $h[n] = 0$ for $n > 0$.

12.32. Let $\mathcal{H}\{\cdot\}$ denote the (ideal) operation of Hilbert transformation; that is,

$$\mathcal{H}\{x[n]\} = \sum_{k=-\infty}^{\infty} x[k]h[n-k],$$

where $h[n]$ is

$$h[n] = \begin{cases} \dfrac{2\sin^2(\pi n/2)}{\pi n}, & n \neq 0, \\ 0, & n = 0. \end{cases}$$

Prove the following properties of the ideal Hilbert transform operator.

(a) $\mathcal{H}\{\mathcal{H}\{x[n]\}\} = -x[n]$

(b) $\sum_{n=-\infty}^{\infty} x[n]\mathcal{H}\{x[n]\} = 0$ [*Hint*: Use Parseval's theorem.]

(c) $\mathcal{H}\{x[n]*y[n]\} = \mathcal{H}\{x[n]\}*y[n] = x[n]*\mathcal{H}\{y[n]\}$, where $x[n]$ and $y[n]$ are any sequences.

12.33. An ideal Hilbert transformer with impulse response

$$h[n] = \begin{cases} \dfrac{2\sin^2(\pi n/2)}{\pi n}, & n \neq 0, \\ 0, & n = 0, \end{cases}$$

has input $x_r[n]$ and output $x_i[n] = x_r[n] * h[n]$, where $x_r[n]$ is a discrete-time random signal.

(a) Find an expression for the autocorrelation sequence $\phi_{x_i x_i}[m]$ in terms of $h[n]$ and $\phi_{x_r x_r}[m]$.

(b) Find an expression for the cross-correlation sequence $\phi_{x_r x_i}[m]$. Show that in this case, $\phi_{x_r x_i}[m]$ is an odd function of m.

(c) Find an expression for the autocorrelation function of the complex analytic signal $x[n] = x_r[n] + jx_i[n]$.

(d) Determine the power spectrum $P_{xx}(\omega)$ for the complex signal in part (c).

12.34. In Section 12.4.3, we discussed an efficient scheme for sampling a bandpass continuous-time signal with Fourier transform such that

$$S_c(j\Omega) = 0 \quad \text{for} \quad |\Omega| \leq \Omega_c \quad \text{and} \quad |\Omega| \geq \Omega_c + \Delta\Omega.$$

The bandpass sampling scheme is depicted in Figure 12.12. At the end of the section, a scheme for reconstructing the original sampled signal $s_r[n]$ was given. The original continuous-time signal $s_c(t)$ in Figure 12.12 can, of course, be reconstructed from $s_r[n]$ by ideal bandlimited interpolation (ideal D/C conversion). Figure P12.34-1 shows a block diagram of the system for reconstructing a real continuous-time bandpass signal from a decimated complex signal. The complex bandpass filter $H_i(e^{j\omega})$ in the figure has a frequency response given by Eq. (12.79).

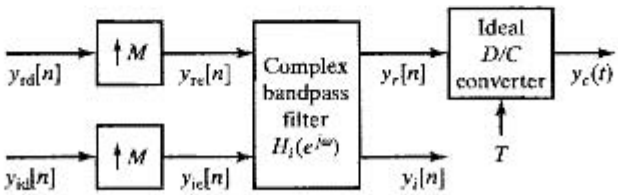

Figure P12.34-1

(a) Using the example depicted in Figure 12.13, show that the system of Figure P12.34-1 will reconstruct the original real bandpass signal (i.e., $y_c(t) = s_c(t)$) if the inputs to the reconstruction system are $y_{rd}[n] = s_{rd}[n]$ and $y_{id}[n] = s_{id}[n]$.

(b) Determine the impulse response $h_i[n] = h_{ri}[n] + jh_{ii}[n]$ of the complex bandpass filter in Figure P12.34-1.

(c) Draw a more detailed block diagram of the system of Figure P12.34-1 in which only real operations are shown. Eliminate any parts of the diagram that are not necessary to compute the final output.

(d) Now consider placing a complex LTI system between the system of Figure 12.12 and the system of Figure P12.34-1. This is depicted in Figure P12.34-2, where the frequency response of the system is denoted $H(e^{j\omega})$. Determine how $H(e^{j\omega})$ should be chosen if it is desired that

$$Y_c(j\Omega) = H_{\text{eff}}(j\Omega)S_c(j\Omega),$$

where

$$H_{\text{eff}}(j\Omega) = \begin{cases} 1, & \Omega_c < |\Omega| < \Omega_c + \Delta\Omega/2, \\ 0, & \text{otherwise.} \end{cases}$$

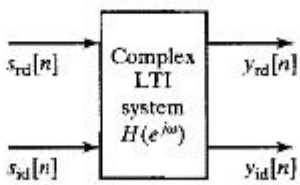

Figure P12.34-2

12.35. In Section 12.3, we defined a sequence $\hat{x}[n]$ referred to as the complex cepstrum of a sequence $x[n]$, and indicated that a causal complex cepstrum $\hat{x}[n]$ is equivalent to the minimum-phase condition of Section 5.4 on $x[n]$. The sequence $\hat{x}[n]$ is the inverse Fourier transform of $\hat{X}(e^{j\omega})$ as defined in Eq. (12.53). Note that because $X(e^{j\omega})$ and $\hat{X}(e^{j\omega})$ are defined, the ROC of both $X(z)$ and $\hat{X}(z)$ must include the unit circle.

(a) Justify the statement that the singularities (poles) of $\hat{X}(z)$ will occur wherever $X(z)$ has either poles or zeros. Use this fact to prove that if $\hat{x}[n]$ is causal, $x[n]$ is minimum phase.

(b) Justify the statement that if $x[n]$ is minimum phase the constraints of the ROC require $\hat{x}[n]$ to be causal.

We can examine this property for the case when $x[n]$ can be written as a superposition of complex exponentials. Specifically, consider a sequence $x[n]$ whose z-transform is

$$X(z) = A\frac{\prod_{k=1}^{M_i}(1 - a_k z^{-1})\prod_{k=1}^{M_o}(1 - b_k z)}{\prod_{k=1}^{N_i}(1 - c_k z^{-1})\prod_{k=1}^{N_o}(1 - d_k z)},$$

where $A > 0$ and a_k, b_k, c_k and d_k all have magnitude less than one.

(c) Write an expression for $\hat{X}(z) = \log X(z)$.

(d) Solve for $\hat{x}[n]$ by taking the inverse z-transform of your answer in part (c).

(e) Based on part (d) and the expression for $X(z)$, argue that for sequences $x[n]$ of this form, a causal complex cepstrum is equivalent to having minimum phase.